

THE NATURE AND DISTRIBUTION OF THE TANTALUM
MINERALS IN THE TANCO (CHEMALLOY) MINE
PEGMATITE AT BERNIC LAKE, MANITOBA.

A Thesis

Submitted to

The Faculty of Graduate Studies

University of Manitoba

In Partial Fulfillment
of the Requirements for the Degree
Master of Science

by

Joel Grice

1970



TABLE OF CONTENTS

<u>CHAPTER</u>	<u>PAGE</u>
ABSTRACT	v
ACKNOWLEDGEMENTS	vii
I. INTRODUCTION	
A. General Introduction	1
B. General Geology of the Tanco Pegmatite	2
C. Previous Work on the Ta Minerals	3
D. Present Study	4
E. Experimental Methods and Discussion of Errors	
(i) Mineral Separation	13
(ii) X-ray Powder Diffraction	14
(iii) Single-Crystal X-ray Diffraction	
Photographs	15
(iv) Electron Probe Microanalysis	16
II. WODGINITE	
A. Introduction	18
B. Physical and Optical Properties	19
C. Chemistry	21
D. Morphological Crystallography	26
E. X-ray Diffraction Examination	29
F. Heating Experiments	39
III. TANTALITE AND PSEUDO-IXIOLITE	
A. Introduction	42
B. Physical and Optical Properties	42
C. Chemistry	43
D. Heating Experiments	47
E. X-ray Diffraction Examination	49
IV. RELATED MINERALS WITHIN THE TANCO PEGMATITE	
A. Tapiolite	57
B. Microlite	57
C. Cassiterite	59
D. Ilmenite	61
V. RELATIONSHIPS BETWEEN THE Ta-OXIDES IN THE TANCO PEGMATITE	
A. Chemical Relationships	64
B. Crystallographic and Structural Relationships	71
VI. GEOLOGICAL IMPLICATIONS	77
REFERENCES	82

LIST OF TABLES

<u>TABLE</u>	<u>PAGE</u>
1. Specimen Details	5
2. Semiquantitative Microprobe Analyses and Chemical Formulae of Wodginites	22
3. Wodginite: Cell dimensions measured from precession photographs	33
4. Cell Dimensions of Wodginites from X-ray Powder Diffractograms	34
5. X-ray Powder Data for Two Wodginites	35
6. Cell Dimensions of Heated Wodginite Specimen G69-2	41
7. Semiquantitative Microprobe Analyses of Tantalites and Pseudo-Ixiolites	44
8. Details of Heating Pseudo-Ixiolites	48
9. X-ray Powder Diffraction Patterns of Pseudo- Ixiolite and Tantalite	53
10. Cell Dimensions of Pseudo-Ixiolites and Tantalites	54
11. Analyses of Some of the Related Minerals	63
12. Orientation Settings of Ixiolite, Tantalite and Wodginite	72

LIST OF FIGURES

<u>FIGURE</u>	<u>PAGE</u>
1. Specimen location map	10
2. Anhedral wodginite grains in partially sericitized K-feldspar	20
3. Euhedral wodginite crystal in partially sericitized K-feldspar	20
4. Electron microprobe x-ray scanning images of wodginite	25
5. Wodginite crystal	27
6. Gnomonic projection of a typical wodginite crystal...	28
7. Stereographic projection of a typical wodginite crystal	28
8. y-axis, zero-level precession photograph of monoclinic wodginite	30
9. x-axis, cone-axis photograph of monoclinic wodginite	31
10. y-axis, cone-axis photograph of monoclinic wodginite	31
11. Plot of splitting between 221 and $\bar{2}21$ peaks versus angle for wodginite	38
12. y-axis, zero-level precession photograph of partially ordered pseudo-ixiolite	51
13. y-axis, zero-level precession photograph of heated pseudo-ixiolite	51
14. x-axis, cone-axis photograph of partially ordered pseudo-ixiolite	52
15. x-axis, cone-axis photograph of heated pseudo-ixiolite	52

<u>FIGURE</u>	<u>PAGE</u>
16. Graph of c versus a -cell dimension for pseudo-ixiolites and tantalites	56
17. Tapiolite associated with wodginite in partially sericitized K-feldspar	58
18. Microlite associated with wodginite in partially sericitized K-feldspar	60
19. Microlite replacing pseudo-ixiolite	60
20. Cassiterite grain in tantalite	62
21. Ternary plot of $(\text{Ta}_2\text{O}_5+\text{Nb}_2\text{O}_5)$, $(\text{SnO}_2+\text{TiO}_2)$ and $(\text{FeO}+\text{MnO})$ in weight percentages	65
22. Weight percent ratios of FeO/MnO versus $\text{Ta}_2\text{O}_5/\text{Nb}_2\text{O}_5$ for wodginite, tantalite, pseudo-ixiolite and microlite	66
23. Electron microprobe x-ray scanning images	69
24. Cell volumes (ixiolite cell) versus weight ratios $(\text{FeO}+\text{SnO}_2+\text{TiO}_2)/\text{MnO}$ for wodginites, tantalites and pseudo-ixiolites	70
25. X-ray powder diffractogram of pseudo-ixiolite, tantalite and wodginite	73
26. Wodginite in typical K-feldspar-quartz-beryl environment	78
27. Tantalite and possibly wodginite in aplitic albite near quartz contact	79
28. Interstitial grain in aplitic albite	80

ABSTRACT

Wodginite $(\text{Ta}, \text{Nb}, \text{Mn}, \text{Fe}, \text{Sn}, \text{Ti})_2\text{O}_4$, manganotantalite $(\text{Mn}, \text{Fe}) (\text{Ta}, \text{Nb}, \text{Ti}, \text{Sn})_2\text{O}_6$ and pseudo-ixiolite $(\text{Ta}, \text{Nb}, \text{Mn}, \text{Fe}, \text{Sn}, \text{Ti})_2\text{O}_4$ are the three major Ta-oxides occurring in the Tanco pegmatite at Bernic Lake, Manitoba, wodginite being by far the most abundant. Microlite $\text{Ca}_2\text{Ta}_2\text{O}_6(\text{O}, \text{OH}, \text{F})$ and tapiolite $(\text{Fe}, \text{Mn}) (\text{Ta}, \text{Nb})_2\text{O}_6$ occur in minor amounts.

A detailed crystallographic study was carried out on the three major Ta-oxides which are closely related crystallographically. Orthorhombic pseudo-ixiolite has the simplest cell ($a=4.76$, $b=5.75$, $c=5.16\text{\AA}$). Upon heating to 1000°C for several hours over a range of oxygen fugacities, the pseudo-ixiolites are converted to orthorhombic tantalites with the a -period three times that of pseudo-ixiolite and with a small increase in comparative a -dimension, with b remaining constant and c decreasing slightly. This change from pseudo-ixiolite to tantalite is considered to result from disordering-ordering of the cations but x-ray photographs show that the two phases are not completely disordered or ordered. The monoclinic wodginites have a marked subcell similar to that of ixiolite but a few weak reflections indicate that the a and b cell dimensions are doubled. The small monoclinic distortion of wodginite from the orthorhombic

ixiolite cell is expressed by a variation in β from $90^{\circ}56'$ to $91^{\circ}6'$ in the Tanco pegmatite specimens studied. All available published data were used to determine the variation of β with the separation of one pair of the major peaks, and a linear equation derived.

The wodginites generally have lower Mn and higher Fe, Sn and Ti contents, and higher Ta/Nb ratios than either tantalite or pseudo-ixiolite. The chemical distinctions between tantalites and pseudo-ixiolites are less marked. Both have low Fe and high Mn, and five out of six tantalites have lower Sn and Ti contents and higher Ta/Nb ratios than the pseudo-ixiolites.

The Ta-minerals occur in distinct zones within the pegmatite. The pseudo-ixiolite occurs in the quartz-plagioclase-K-feldspar-spodumene-muscovite- zone and wodginite occurs in the K-feldspar-muscovite-plagioclase-quartz-beryl zone just inside the pseudo-ixiolite bearing zone. The albitic aplite contains both tantalite and wodginite. The zoning of these Ta-minerals within the pegmatite is discussed in relation to the paragenesis of the body.

ACKNOWLEDGEMENTS

The author is very grateful to Dr. R.B.Ferguson, Professor of Mineralogy at the University of Manitoba, for the suggestion of this project and continued guidance throughout the research.

Mr. C.T.Williams, Mine Manager and Mr. R.A.Crouse, Geologist of the Tanco Mine at Bernic Lake, Manitoba, were very helpful in making specimen collection within the mine possible.

The electron micro-probe at the Whiteshell Nuclear Research Establishment in Pinawa, Manitoba was made available through the generosity of Dr. A.Sawatzky of the Material Sciences Branch. A special thanks to Mr. S.Jones, the probe operator at Pinawa for his time spent on the analyses in this thesis. Dr. J.C.Rucklidge and Miss E. Gasparrini, Geology Department, University of Toronto were kind enough to provide two electron probe analyses.

Two computer programs were used in this project: Dr. D.B.Stewart of the United States Geological Survey, Washington, D.C. provided a copy of Appleman, Handwerker and Evans' program for the least squares refinement of unit cell dimensions from powder diffraction data; and Dr. J.C. Rucklidge provided a copy of the program written by himself and Miss E. Gasparrini for reduction of electron probe data.

Members of the Earth Sciences staff at the

University of Manitoba whom the author would like to thank are Dr. P.Cerny for valuable advice and discussions, Dr. A.C. Turnock for assistance with heating experiments, Miss I. Berta for the preparation of polished and thin sections, and Mr. R. Pryhitko for photographs.

Financial assistance was provided in part through Dr. R.B.Ferguson by means of research grants from the Geological Survey of Canada and the National Research Council, and in part by a University of Manitoba Summer Stipend.

CHAPTER I. INTRODUCTION

(a) General Introduction

The Tanco (Chemalloy) Li-Cs-Ta-Be pegmatite is located on the western part of Bernic Lake approximately 100 miles northeast of Winnipeg. This body is part of the southeastern Manitoba pegmatite district.

The property was first staked in 1929 by Jack Nutt Tin Mines Limited for a cassiterite occurrence. In 1954 Montgary Explorations Limited, now Chemalloy Minerals Limited, took over the property. Chemalloy marketed small tonnages of quartz, and stockpiled various minerals. In 1962 the mine was abandoned and allowed to flood. In 1967 Tantalum Mining Corporation reopened the mine and set up equipment for mining and concentrating tantalum-oxide ore.

From previous work it was known that tantalite, wodginite and minor amounts of microlite and tapiolite were present in the mine. Due to the current interest in the Tanco pegmatite as a tantalum mine, it appeared that it would be valuable to fully define the Ta-minerals there and to do a detailed chemical and crystallographic study of these minerals in relation to their position in the pegmatite.

Concurrent studies in the Mineralogical Laboratory at the University of Manitoba on other minerals in this pegmatite are: petalite, spodumene, and feldspars by Postdoctoral Fellow Dr. P. Černý; amblygonite-montebrazite

by M.Sc. candidate Mrs. Iva Černá; and Li-Rb-Cs micas by M.Sc. candidate Mr. Romano Rinaldi. The accumulated information from these and the author's studies should give evidence of the pegmatite paragenesis at Bernic Lake.

(b) General Geology of the Tanco Pegmatite

The Tanco pegmatite was first described in detail by Hutchinson (1959) and later by Wright (1963) under the name Montgary pegmatite. It is essentially Wright's work which is being used in this general description.

The pegmatite body has the shape of a flat-lying, elongate disc. The north-south axis is about 1,500 feet long, the east-west dimension is at least one-half mile long, and the thickness reaches a maximum of 280 feet. It dips north at 10° - 15° . The body is enclosed in Precambrian amphibolite with large neighbouring bodies of granite to the south and west.

The Tanco pegmatite is complexly zoned. Wright (1963) proposed six zones: (1) a quartz-albite border zone; (2) a perthite-quartz-plagioclase-muscovite wall zone; (3) a spodumene-perthite-plagioclase-quartz intermediate zone; (4) a spodumene-quartz intermediate zone with minor perthite; (5) a microcline-quartz intermediate zone, and (6) a quartz core. In addition to these six zones is an aplitic albite, a fine-grained lepidolite and a pollucite which Wright

suggests are late-stage replacement bodies. Jahns and Burnham (1969) on the other hand have suggested that aplitic albite in pegmatites of this type is a primary magmatic phase formed early in the pegmatite's history.

The Ta-minerals occur in Wright's zones 3,4 and 5 and in the aplitic albite and the lepidolite bodies which are also regarded as zones in this thesis. Also in this thesis Wright's zones 3 and 4 are combined and called the quartz-plagioclase-spodumene-K-feldspar-muscovite zone; and Wright's zone 5 is termed the K-feldspar-muscovite-plagioclase-quartz-beryl zone.

(c) Previous Work on the Ta Minerals

Although considerable mineralogical work has been done on wodginite, tantalite, pseudo-ixiolite, tapiolite and microlite from various localities throughout the world only a limited amount of mineralogical research has been published on the Ta minerals at Bernic Lake. Bernic Lake wodginite was one of the first wodginites reported (Nickel et al., 1963a). Nickel et al. (1963b) also described the crystallographic relationships between wodginite, tantalite and pseudo-ixiolite. The Tanco Company have done considerable drilling and analyzing to determine the grade and extent of their Ta ore but no data as of yet has been published.

(d) Present Study

The Tanco (Chemalloy) pegmatite is a single body from which mutually-occurring wodginite, tantalite and pseudo-ixiolite could all be collected and studied. Tapiolite, microlite, cassiterite and ilmenite also occur in this pegmatite in small amounts, and minor observations were made on these minerals.

Sixty-five oxide-bearing rock specimens were collected in the mine, and an additional five specimens were contributed to this study by Dr. P. Černý. Table 1 gives a complete listing of the specimens and Fig. 1 gives their location in the mine. Table 1 also outlines the study made on each specimen. Initially the oxides from each specimen were run on the x-ray powder diffractometer (column 4) to try and identify as many phases as possible. Eighteen thin-sections (column 9) and forty-three polished sections (column 10) were made of specimens throughout the mine. Several wodginites, tantalites and pseudo-ixiolites were examined by single-crystal x-ray diffraction (column 7), and accurate cell dimensions were determined on all but one of these by x-ray powder diffraction (column 8). These specimens and some others were analyzed by electron probe (column 6). The specimens for which a detailed study was

Table 1. Specimen Details

NOTE: 1. Abbreviations used:

Silicate Minerals

Ab	Albite
Ap	Aplitic albite
Bl	Beryl
Cl	Cleav ^e landite
KF	K-feldspar
Ms	Muscovite
Q	Quartz
Sp	Spodumene

Oxide Minerals

C	Cassiterite
M	Microlite
PI	Pseudo-ixiolite
T	Tantalite
Tp	Tapiolite
W	Wodginite

NOTE: 2. Zone numbers:

- 1 Quartz - plagioclase-spodumene-K-feldspar-muscovite.
- 2 K-feldspar-muscovite-plagioclase-quartz-beryl.
- 3 Aplitic albite.

Table 1. - continued

1 Specimen No.	2 Matrix Minerals	3 Zone	4 X-ray Powder Ident.	5 Ident. by probe(*) or optics	6 Analyzed by probe	7 X-ray Precession	8 Cell Dimensions	9 Thin Section	10 Polished Section	11 Remarks
G69-1	KF, Ms, Q, Bl	2	W	M				3	2	Sphene
-2	KF, Ms, Q	2	W		X	X	X			
-3	KF, Q, Ms	2	W							
-4	KF, Ms	2	W							
-5	KF, Ms	2	W							
-6	KF, Ms	2	W							Found adjacent to zone 3, pattern like reduced W
-7	Ap, Ms	3	W, T						3	X-ray pattern like reduced W
-8	KF-Ap	2/3	T	W	X				2	
-9	KF	2	C, W							Lepidolite
-10	KF, Ms, Q, Sp	2	-	C					1	
-11	KF, Q, Ms, Ab	2	W	M				1	1	Contact zone 2 and Q core
-12	KF, Ms, Q	2	W							
-13	KF, Ms, Q	2	W, T		X	X	X			Apatite
-14	KF, Ms, Q	2	W							
-15	KF, Ms, Ab	2	W							
-16	Ap, Q, Ms	3	W, T							
-17	KF, Q	2	W		X	X	X		1	
-18	KF, Ms	2	W							
-19	KF, Ms, Bl, Q	2	W	M	X			1	2	
-20	KF, Ms, Q	2	W						1	
-21	KF, Ms, Q	2	W, T	M	X			1	2	

Table 1. - continued

1 Specimen No.	2 Matrix Minerals	3 Zone	4 X-ray Powder Ident.	5 Ident. by probe (*) or optics	6 Analyzed by probe	7 X-ray Precession	8 Cell Dimensions	9 Thin Section	10 Polished Section	11 Remarks
G69-22	KF, Ms, Q	2	W						1	
-23	KF, Q, Ms	2	W							
-24	KF, Ms, Q	2	W					2	3	
-25	KF, Bl, Q	2	W							
-26	Q, KF, Ms	2	C							C in streaks
-27	KF	2	C, W							
-28	KF	2	W							Near bluish Ap
-29a	Ap-Q	3	T							
-29b	Ap-Q	3	T		X	X	X	1	5	
-30	Q, Cl, Ms	1	PI	M*	X				1	Apatite
-31	Q, Cl, Ms	1	PI, M	M*	X		X		1	
-32	Ap, KF, Q	3	W, C, T	C					1	
-33	Ms, KF, Q	2	W							
-34	KF, Q, Ms	2	W							
-35	KF, Ms	2	W							
-36	KF, Ms	2	W							
-37	KF, Ms	2	W						1	
-38	KF, Ms, Q/Ap	2/3	W, T							
-39	Kf, Ms	2	W		X	X	X		1	
-40	Q, KF	1	-							Tourmaline, Apatite
-41	Ms, KF, Q	2	W							

Table 1. - continued

1 Specimen No.	2 Matrix Minerals	3 Zone	4 X-ray Powder Ident.	5 Ident. by probe(*) or optics	6 Analyzed by probe	7 X-ray Precession	8 Cell Dimensions	9 Thin Section	10 Polished Section	11 Remarks
G69-42	KF, Ms, B1, Q	2	W							
-43a	Ap, Q	3	W, M	M				1	3	
-43b	KF, Ms	2	Tp, W, M	M, Tp				2	2	
-44	KF, Ms, Q, B1	2	W		X			2	2	
-45	KF, Ms, Q	2	W							
-46a	KF, Ms, B1, Q	2	W		X			1	2	
-46b	KF, Ms	2	W		X				1	
-47	Ap, Ms, Q	3	W, T							
-48	KF, Ms, Q	2	W							
-49	KF, Ms	2	W							
-50	KF, Ms, Q	2	W							
-51	KF, Ms	2	W							
-52	KF, Ms, Q	2	T, W, Tp	M	X			2	3	
-53	Ap, Q	3	T		X	X	X			
-54	Q, Cl	1	PI							
-55	Cl, Q, Ms	1	PI		X	X	X			
-56	Q, Sp, Ab	1	PI							
-57	Ap, Q	3	W							
-58	Q, Ms, Ab	1	T/PI		X	X	X			Adjacent to zone 3
-59	Cl, Q, Sp, Ms	1	PI, C		X			1	1	

Table 1. - continued

1 Specimen No.	2 Matrix Minerals	3 Zone	4 X-ray Powder Ident.	5 Ident. by probe (*) or optics	6 Analyzed by probe	7 X-ray Precession	8 Cell Dimensions	9 Thin Section	10 Polished Section	11 Remarks
G69-60	Q, Cl	1	PI		X	X	X			
-61	Q, Cl	1	PI		X	X	X			
G70-I	Q, Ab, Ms	1	PI							
-II	Ap/KF, Q	3/2	W, T							
-III	Q, Cl	1	PI							
-IV	Ap/Q, Cl	3/1	PI							
BLM-1A	KF, Q, Ms	2	W		X	X	X			- near G69-14
BLM-16A	Q, KF	1	PI							- west drift
BLM-16C	Ms, Q	2	W, M							- main drift: crystal morphology
BLM-71	Ap, Q	3	C							- near G69-8
BLM-77	Q, KF	1	C							- near G69-40

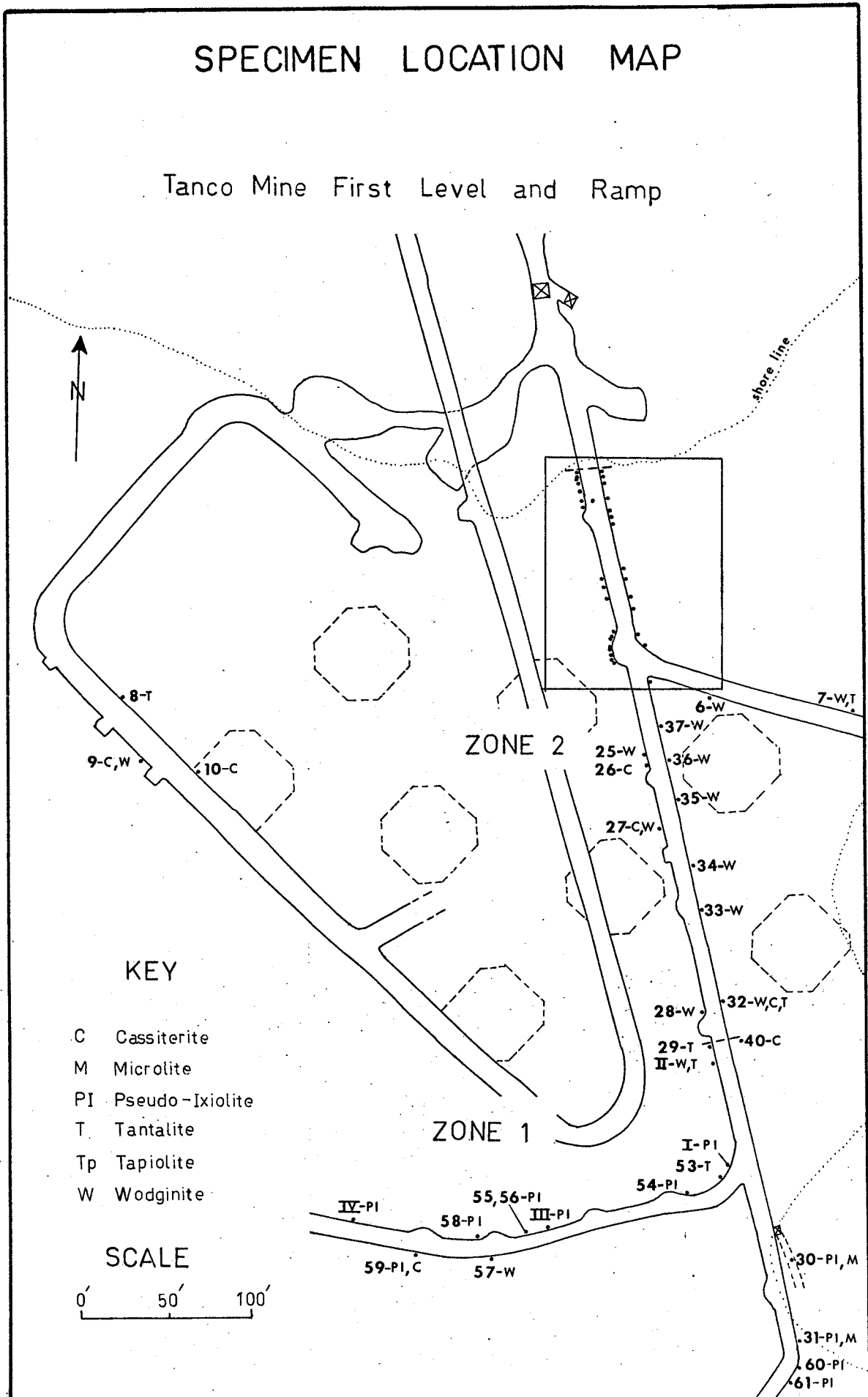
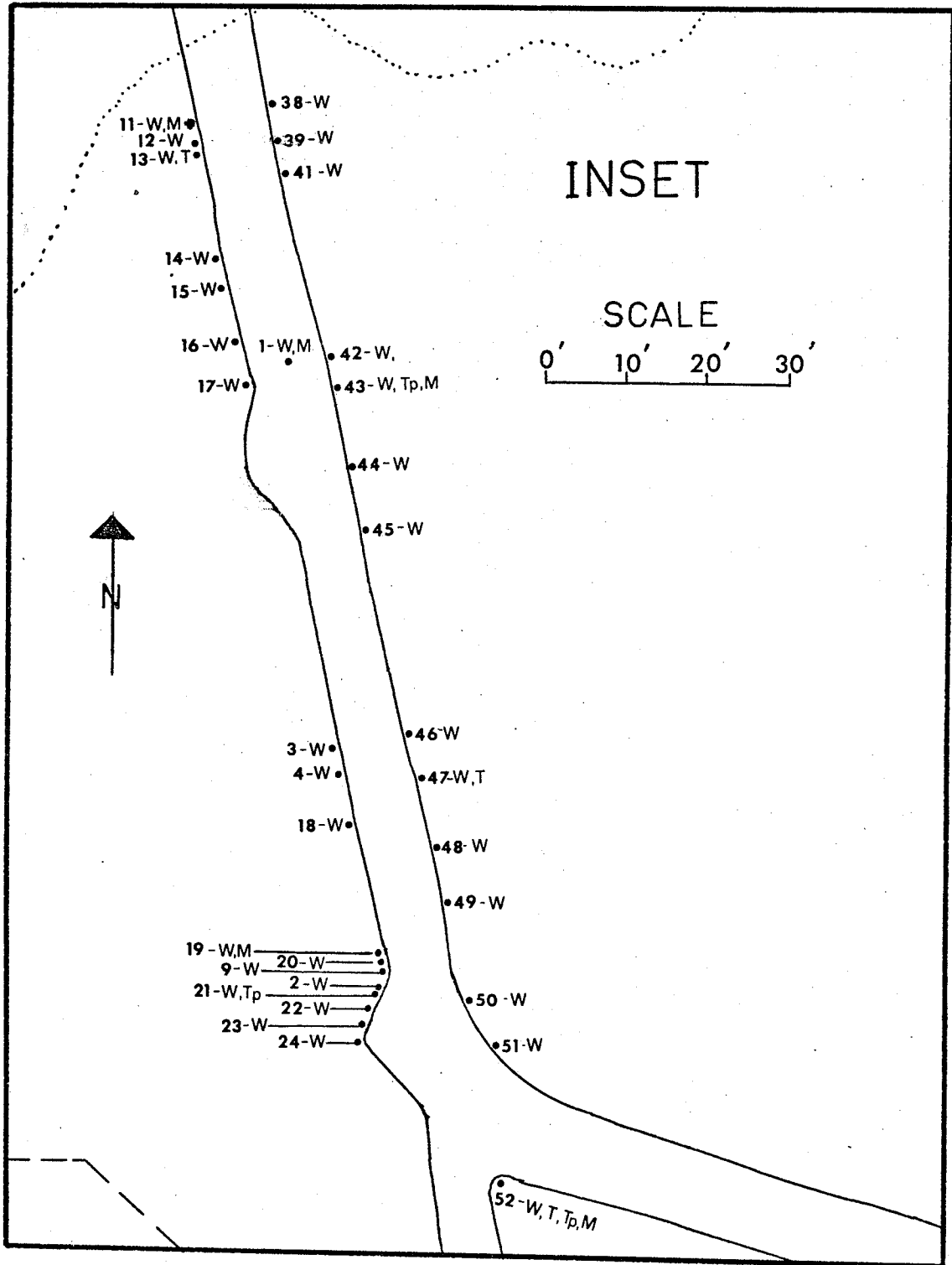


Fig. 1. - continued



carried out were chosen on the basis of location within the pegmatite or because of some interesting feature in the x-ray powder patterns such as differences in peak splitting in wodginites and disordering in tantalites.

The fact that these Ta minerals occur together in the same pegmatite enabled the author and his associates to compare the mineralogy, chemistry and paragenesis of these oxides within a single body of common history.

(e) Experimental Methods and Discussion of Errors

(i) Mineral Separation

When mineral grains for x-ray powder diffractograms or chemical analysis were not easily separable from their matrix by hand picking, heavy liquid separation was used. The sample was crushed and sieved to 100-200 mesh, and bromoform ($\rho=2.9$ gms/cc) was used to separate the heavier minerals. In some instances spodumene and Li-muscovite were removed using the Frantz Isodynamic Separator. It was not possible in practice to separate wodginite, tantalite and cassiterite by the only possible simple method, the Frantz Separator, due to their similar mass susceptibilities -- these minerals all have low iron contents and high specific gravities. This feature became evident when the Mine Manager at Tanco requested a separation of Ta minerals from cassiterite in one of their concentrates to get an idea of the percentage of cassiterite present. The high magnetic side tended to concentrate wodginite and tantalite but the separation was not very effective.

(ii) X-ray Powder Diffraction

The primary instrument used for mineral identification in this study was a standard Philips (Norelco) X-ray powder diffractometer. Each sample was run at a goniometer speed of $\frac{1}{2}^{\circ} 2\theta$ per minute for the 2θ range of 10° to 70° using CuK_{α} radiation and a chart speed of 10X.

The samples for which accurate cell dimensions were derived were run with an internal standard three times on the diffractometer with a scanning speed of $\frac{1}{2}^{\circ} 2\theta$ per minute and a fast chart speed of 20X. This gives a record on the chart which can be read to within $.01^{\circ} 2\theta$. Between each run for any one sample the slide was moved to expose to the x-ray beam a different portion of the powder each time. F.G.Smith (1969) has shown that the largest deviation in peak spacings is brought about by this simple procedure, and it is necessary for accurate results to get average d values.

The 2θ values of the sample peaks were measured relative to those for the internal standard which was synthetic CaF_2 . The synthetic fluorite was treated by (a) heating at 800°C for one hour, (b) grinding, (c) repeating (a) and (b), (d) heating at 500°C overnight, and (e) by a final grinding. Such a treated fluorite yields a cubic cell edge $a=5.4620 \text{ \AA}$ (Stewart in Tilling, 1968). For several runs, reasonably well defined peaks gave a standard deviation of $\pm .02^{\circ} 2\theta$.

The 2θ values measured in this manner were used in the computer program of Appleman et al. (1963) for a least squares refinement of the unit cell dimensions. A weighting factor was applied to each reflection on the basis of its clarity and reproducibility between runs. The maximum tolerance for matching calculated with observed 2θ values was set for $\pm .04^\circ 2\theta$. This allows $\pm .02^\circ 2\theta$ in measuring the peaks of both the internal standard and the sample. The errors quoted later for each cell dimension are standard errors about the mean calculated for each reflection accepted.

(iii) Single-Crystal X-ray Diffraction Photographs

Single-crystal x-ray photographs were taken with MoK α radiation on two different precession instruments, an Otto von der Heyde and a Charles Supper. The Supper instrument was equipped with a Polaroid attachment which reduced the time required to orient the crystals. It was found that setting pictures could be taken with approximately one-eighth the exposure time required for regular Estar base x-ray film.

Cell dimensions were derived from zero-level precession photographs which were measured using a mm. scale with attached vernier. The errors quoted later are standard deviations about the mean. Neither precession instrument had been calibrated, and consequently these errors were those of measurement precision.

(iv) Electron Probe Microanalysis

Through the generosity of Dr. A.Sawatzky at the Whiteshell Nuclear Research Establishment in Pinawa, Manitoba an electron probe was made available. Mr. S.Jones, the probe operator at Pinawa is primarily responsible for most of the chemical analyses in this thesis.

A Philips AMR/3 microprobe was used. Operating conditions were:

electron accelerating voltage	30kV
beam current	48 ma
sample current	.1-.2 ma
gas mixture in proportional counters	90%A,10%methane
detector voltage	1.7kV
take-off angle	15° 20'
analysing crystal	mica

The standards used were metals of the pure elements. The metallic elements analyzed for and the wavelengths used were:

Ti 3 rd order K _α	Nb 2 nd order L _β
Mn 3 rd order K _α	Sn 3 rd order L _α
Fe 5 th order K _α	Ta 7 th order L _α

Scandium was not detected in two of the samples which were tested for this element. For each element 5 counts were taken with a duration of 20 seconds each. Care was taken to

count on exactly the same spot each time by burning the sample with the beam.

The intensity data from the electron probe were refined using a computer program, EMPADR VII, written by J.C.Rucklidge and E.L.Gasparrini (1969). Essentially the program does a least squares correction of measured concentration for (a) dead time, (b) atomic number, (c) absorption, and (d) fluorescence.

Due to the nature of the standards and the number of the elements involved, (bringing about more possibilities of interference), the author regards the error in the probe analyses as about $\pm 5\%$ of the value quoted. Unfortunately no accurate measurement of the true error could be made as no chemically similar oxide of known composition was available. Within the five counts for each element the variance was generally less than .5% except for Nb for which only a weak L_{β} peak could be used; for this the variance was approximately 1.5%.

CHAPTER II. WODGINITE

(a) Introduction

Wodginite was first described as a new mineral by E.H.Nickel, J.F.Rowland and R.C.McAdam in 1963. The mineral was first discovered at Wodgina, Australia and the name wodginite was given by these authors in recognition of the locality. In the same paper, they described wodginite at the Chemalloy (now the Tanco) pegmatite. Since that time several other wodginite occurrences have been described: Rwanda, Belgium (Bourguignon and Mélon, 1965); Krasonice, Moravia (Luna, 1965); Kalbin Range, U.S.S.R. (Khvostova et al., 1965); Sukula, Tammela, S.W. Finland (Vorma and Siivola, 1967); Karibib, Southwest Africa (von Knorring, 1968); and Ankole, S.W. Uganda (von Knorring, Sahama and Lehtinen, 1969).

The mineral is monoclinic and was originally reported as a tin-manganese tantalite. Turnock (1965) showed that tin is not an essential component of synthetic wodginite and that the phase change from orthorhombic tantalite to wodginite was obtained by an increase in oxygen fugacity.

(b) Physical and Optical Properties

The wodginites found at Bernic Lake, Manitoba usually occur as poorly formed, sugary crystals (Fig. 2), some show a prismatic crystal habit (Fig. 3) but rarely do they occur as well-developed crystals (Fig. 5). The colour varies from reddish-brown in the granular variety to almost black in well-developed crystals; all have a pale red-brown streak.

In transmitted light wodginite is very highly coloured in shades of orange-brown. Grains are usually anhedral. They have a high relief ($n \gg 1.54$) and a high birefringence. When it was possible to get a figure on a wodginite grain, it was biaxial positive.

In reflected light wodginite is grey when viewed in air with a blue filter. Under crossed polars it is slightly anisotropic and displays a strong internal reflection, similar to the red-brown internal reflection of tantalite.

Fig.2. Anhedral wodginite grains in partially sericitized K-feldspar. Transmitted light, plane polarized, X35.

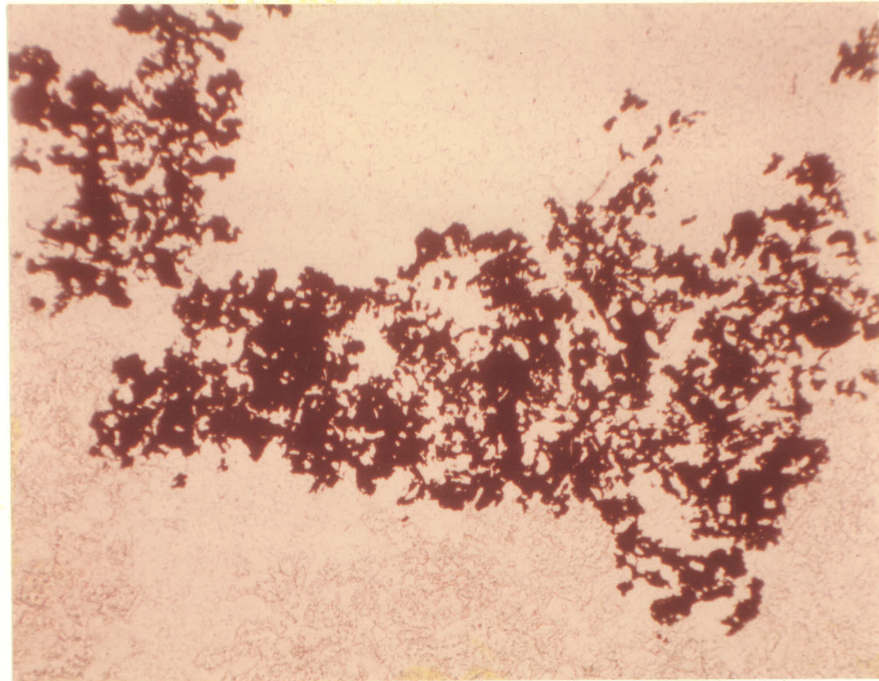
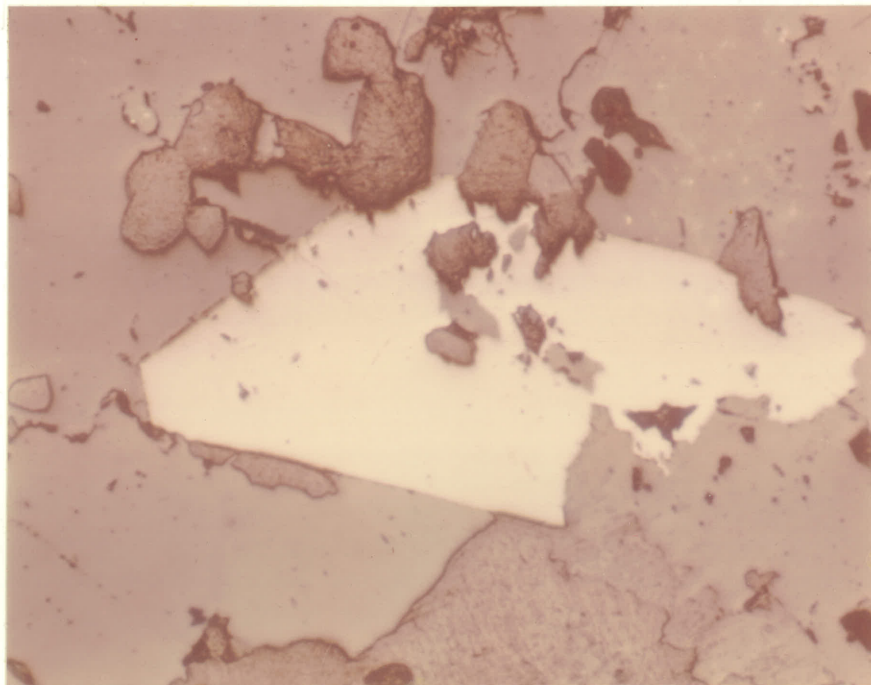


Fig.3. Euhedral wodginite crystal in partially sericitized K-feldspar. Reflected light, plane polarized, X120.



(c) Chemistry

Several semi-quantitative electron microprobe analyses were done and the results are shown in Table 2. An 'S' in the specimen number indicates that the crystal was used in the single-crystal x-ray precession work. Fe is arbitrarily reported as FeO since no ferrous-ferric determination could be made. The analyses have high totals. These high totals may be due to the SnO₂ values because when cassiterite was analyzed using pure Sn metal as a standard, the analysis gave approximately 105% SnO₂. The reason for this is not known. Gasparrini, the probe operator at the Department of Geology, University of Toronto, was good enough to do two analyses on specimen G69-46A. She also found her total weight percent of the oxides was greater than 100%.

The probe showed that even within a single grain there are heterogeneities in wadginites: an example of this is shown in analysis G69-46A-- two analyses are given (-46A1 and -46A2) for two spots within the same grain. Gasparrini probed the same grain but not necessarily the same areas of this grain as Jones and also found the mineral quite variable in composition. The heterogeneity of wadginite is also shown in Fig.4 which consists of three electron probe x-ray scans. The Ta and Mn x-ray

Table 2. Semiquantitative Microprobe Analyses and Chemical Formulae of Wodginites

Analyses in Weight Percent

Specimen No.	G69-S2	G69-8I	G69-S13	G69-17	G69-S17
MnO	10.4	8.9	10.0	10.8	9.2
FeO	1.0	3.3	1.2	1.0	3.0
SnO ₂	15.7	14.7	13.9	14.2	15.5
TiO ₂	3.8	3.2	3.8	2.7	1.3
Ta ₂ O ₅	71.8	66.9	72.9	74.5	73.3
Nb ₂ O ₅	1.0	5.5	1.0	0.5	1.0
Total	103.7	102.5	102.8	103.7	103.3

Numbers of Cations on the Basis of 32(0)

Mn ⁺²	3.63	3.07	3.52	3.85	3.09
Fe ⁺²	.34	1.12	.42	.35	.99
Sn ⁺⁴	2.58	2.39	2.30	2.38	2.45
Ti ⁺⁴	1.18	.98	1.19	.86	1.40
Ta ⁺⁵	8.04	7.41	8.24	8.43	7.91
Nb ⁺⁵	.16	1.01	.18	.09	.18
Total	15.93	15.98	15.85	15.96	16.02

Table 2. - continued

Table 2. - Continued

Analyses in Weight Percent

<u>Specimen No.</u>	<u>G69-19I</u>	<u>G69-21I</u>	<u>G69-S39</u>	<u>G69-44II</u>	<u>BLM-S1A</u>
MnO	9.4	8.3	9.8	9.2	9.1
FeO	2.7	5.2	2.1	2.8	2.9
SnO ₂	14.0	17.0	15.4	18.9	15.2
TiO ₂	2.5	0.2	4.0	1.2	4.0
Ta ₂ O ₅	75.3	69.1	70.2	69.4	69.3
Nb ₂ O ₅	0.2	2.7	1.5	2.0	2.0
Total	104.1	102.5	103.0	103.5	102.5

Numbers of Cations on the Basis of 32(O)

Mn ⁺²	3.31	2.99	3.46	3.26	3.18
Fe ⁺²	.94	1.85	.73	.98	1.00
Sn ⁺⁴	2.32	2.87	2.56	3.15	2.50
Ti ⁺⁴	.78	.07	1.25	.38	1.29
Ta ⁺⁵	8.53	7.94	7.96	7.90	7.77
Nb ⁺⁵	.08	.55	.11	.38	.37
Total	15.96	16.27	16.07	16.05	16.11

Table 2. - continued

Table 2. - Continued

Analyses in Weight Percent

Specimen No.	<u>G69-46A1</u>	<u>G69-46A2</u>	<u>*G69-46A1</u>	<u>*G69-46A2</u>	<u>G69-46B</u>
MnO	12.0	12.0	9.7	9.8	10.4
FeO	3.2	3.8	4.9	5.2	2.0
SnO ₂	15.1	14.5	15.8	10.1	15.9
TiO ₂	4.0	4.8	0.7	3.0	5.4
Ta ₂ O ₅	68.7	64.0	68.2	72.7	68.0
Nb ₂ O ₅	0.5	5.0	3.3	3.6	2.0
Total	103.5	104.1	102.6	104.4	103.7

Numbers of Cations on the Basis of 32(0)

Mn ⁺²	4.17	4.01	3.48	3.38	3.55
Fe ⁺²	1.10	1.25	1.74	1.77	.68
Sn ⁺⁴	2.47	2.25	2.67	1.63	2.05
Ti ⁺⁴	1.23	1.42	.22	.92	1.64
Ta ⁺⁵	7.66	6.87	7.86	8.38	7.47
Nb ⁺⁵	.03	.89	.64	.66	.30
Total	16.66	16.69	16.61	16.74	15.69

Analyst Mr. S. Jones, Nuclear Research Establishment, Pinawa
for all specimens except those marked by an asterisk *.

***Analyst** Miss E. Gasparri, Department of Geology, University
of Toronto.

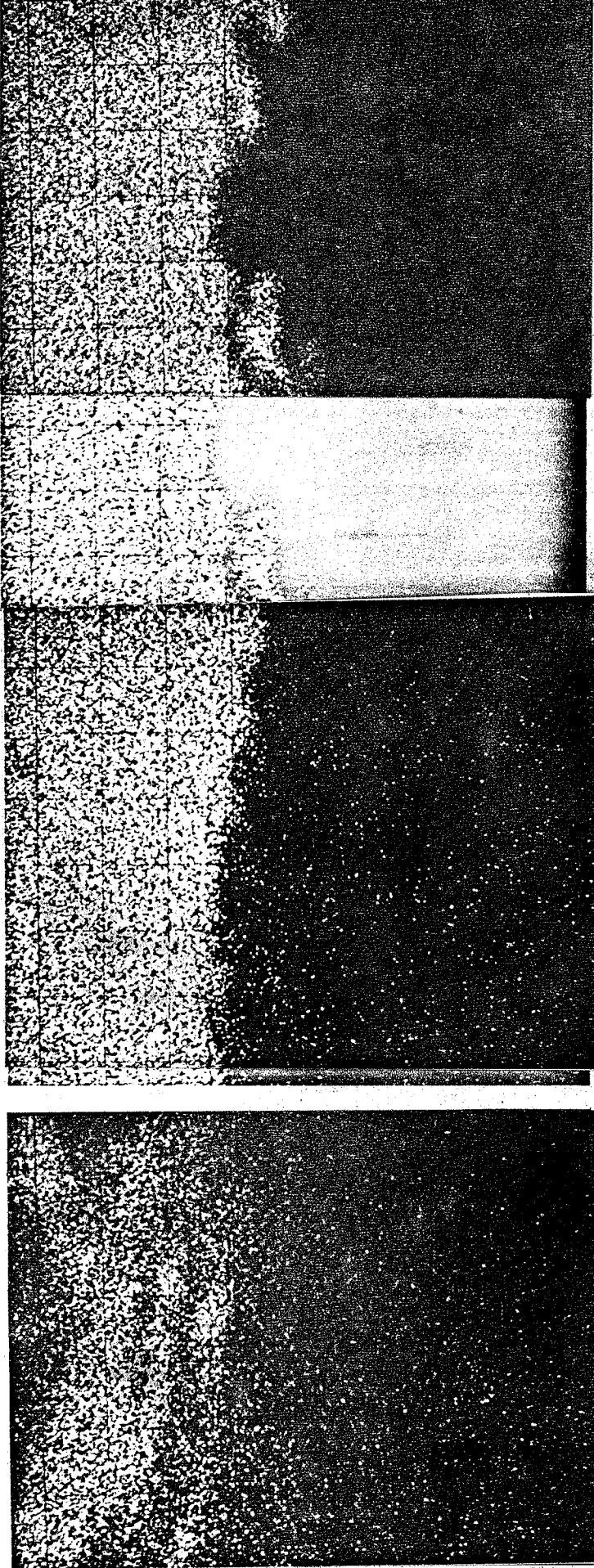


Fig.4. Electron Microprobe x-ray scanning images. Wodginite grain on the left and silicate on the right. Notice the even distribution of Ta and Mn but the heterogeneity of Sn in the wodginite.

Ta-Scan

Mn-Scan

Sn-Scan

50 μ

scans have a fairly even distribution except along the wodginite-silicate boundary whereas the Sn scan is quite heterogeneous.

Table 2 shows that the Bernic Lake wodginites are generally rich in Mn, Sn, Ta, and for these minerals in Ti; and poor in Fe and Nb. A comparison of the chemistry of all the Ta minerals at Bernic Lake will be discussed in the last chapter. The chemical formulae given for each analysis is of the type $A_{16}O_{32}$ where A represents the metal ions Ta, Nb, Mn, Fe, Sn and Ti. The totals of the cations in most cases agrees well with the formulae given above.

(d) Morphological Crystallography

Two wodginite crystals were mounted and measured on the reflecting goniometer. The crystals have the habit shown in Fig. 5. The gnomonic projection for a typical crystal is shown in Fig. 6 and the stereographic projection in Fig. 7. The dominant forms are $\{111\}$, $\{11\bar{1}\}$, $\{001\}$, $\{10\bar{1}\}$, $\{10\bar{1}\}$ and $\{010\}$; $\{031\}$, $\{335\}$ occur as subordinate forms. The orientation of wodginite is that of Nickel et al. (1963a) and given in Strunz and Tennyson (1966, p.187).

Fig.5. Wodginite Crystal (Specimen BLM-16C): Typical habit.

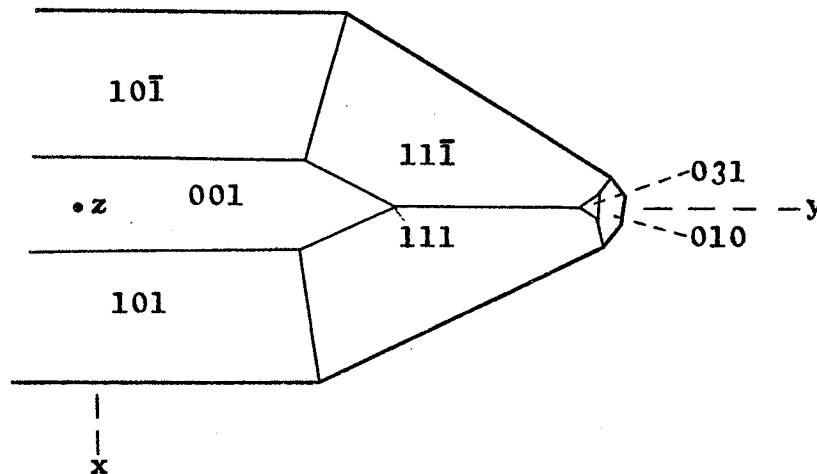


Fig.6. Gnomonic Projection of a Typical Wodginite Crystal

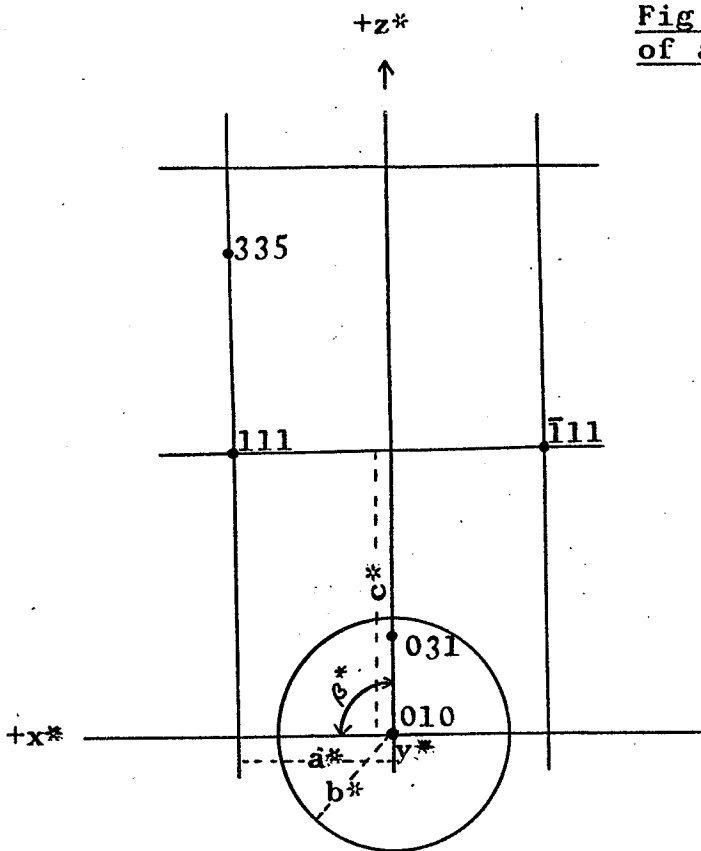
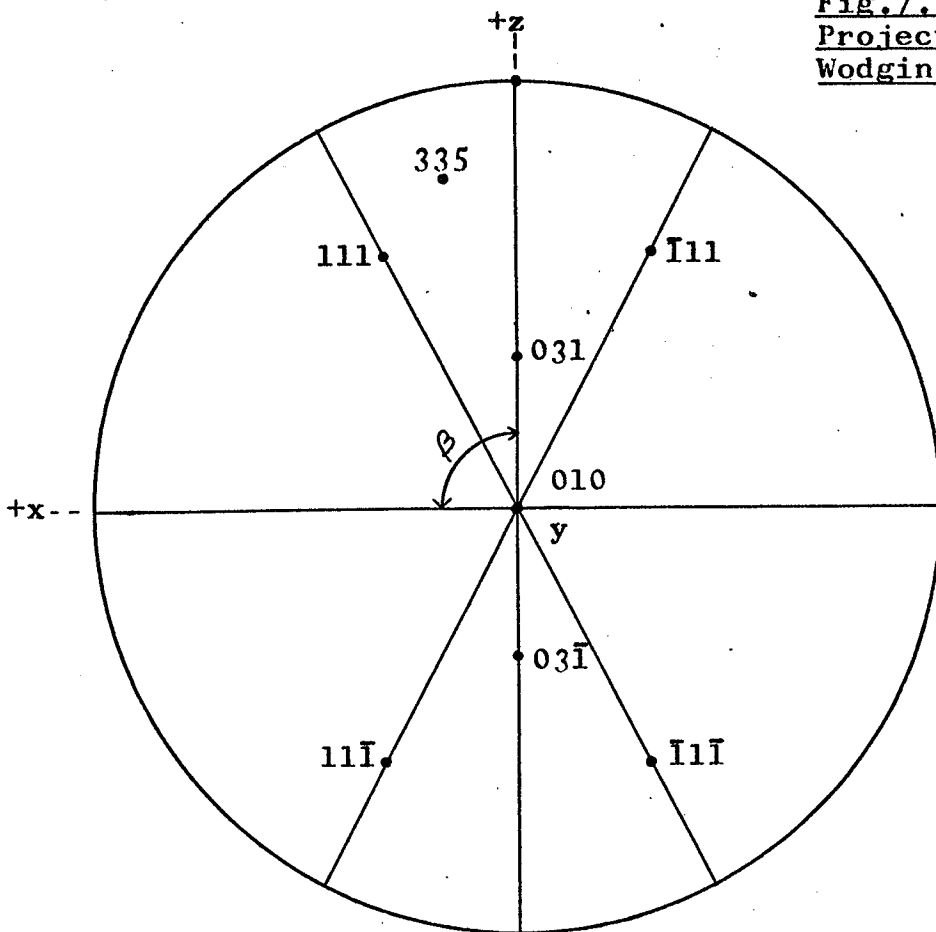


Fig.7. Stereographic Projection of a Typical Wodginite Crystal



(e) X-ray Diffraction Examination

About 50 wadginite samples from Bernic Lake were x-rayed on the powder diffractometer. From these runs five samples were chosen for closer study by detailed powder and by single-crystal x-ray methods. The choices were made on the basis of apparent lattice spacing and intensity variations, both of which were, however, very slight.

The single-crystal precession work revealed the following:

Diffraction Symmetry : Monoclinic 2/m
Extinction Conditions: hkl only with $h+k=2n$
 h0l only with $h=2n, l=2n$
Space Group : C 2/c or Cc

Using the settings of Nickel et al. (1963a) the space group they determined was confirmed by this work.

Fig.8 is a 0-level, y-axis precession photograph which shows the small departure from a right angle of β^* ($\beta^* \approx 89^\circ$), and the occurrence of the h0l reflections only with h even and l even. Cone-axis photographs (Figs. 9&10) about the x- and y-axes show a strong repeat halved by only a few weak reflections giving a true cell with

$$a \approx 9.5 \text{ \AA}, b \approx 11.4 \text{ \AA}, \text{ and } c \approx 5.1 \text{ \AA},$$

and a strong pseudo-cell with

$$a \approx \frac{1}{2} \times 9.5 \text{ \AA}, b \approx \frac{1}{2} \times 11.4 \text{ \AA}, \text{ and } c \approx 5.1 \text{ \AA}.$$

The true cell is that given by Nickel et al. (1963a), but

Fig. 8. y-axis, zero-level precession photograph of monoclinic wadginite. Natural size, $F=60\text{mm}$, $\bar{\mu} = 25^\circ$, MoK_α radiation/Zr filter.

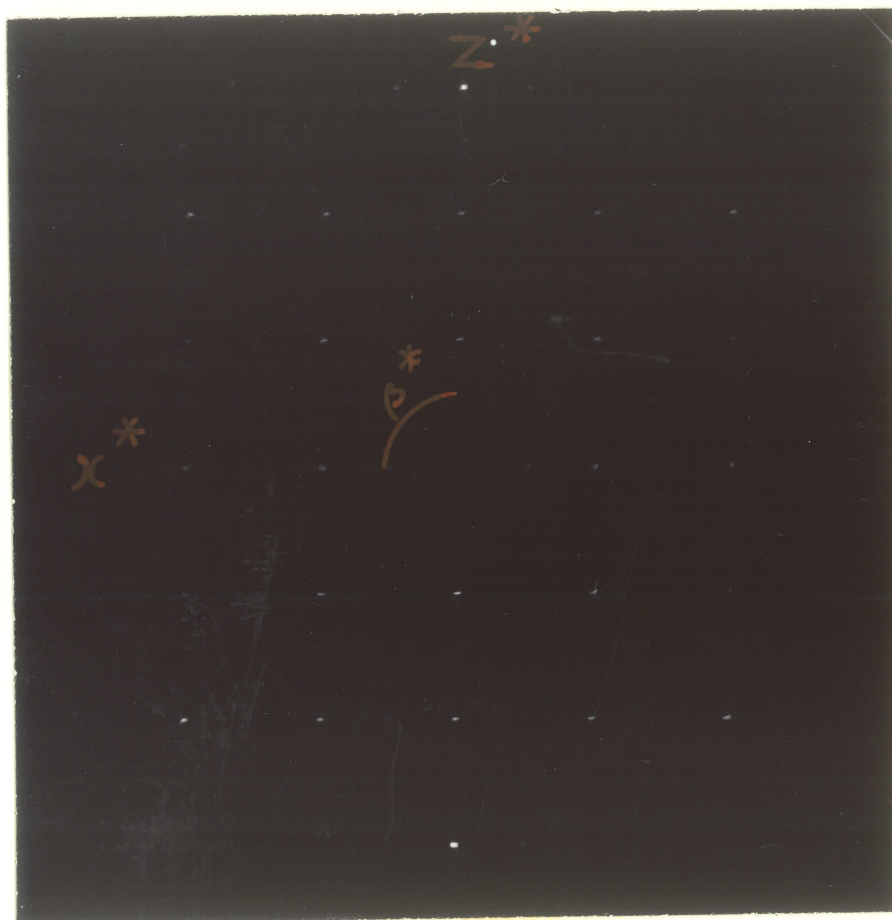


Fig. 9. x-axis, cone-axis photograph of monoclinic wodginite. Natural size, $F=60\text{mm}$, $s=32\text{mm}$, $\bar{\mu}=10^\circ$, MoK_α radiation/Zr filter. Note the few weak reflections which double the a-cell dimension.

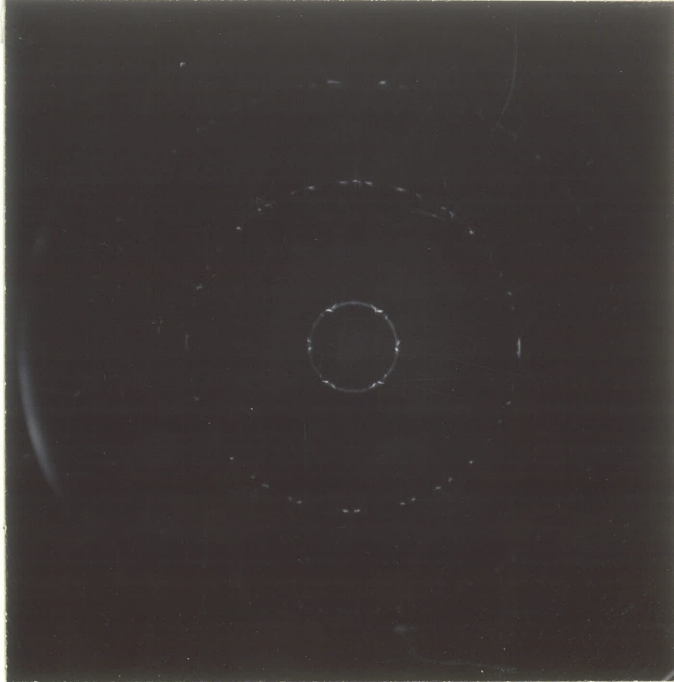
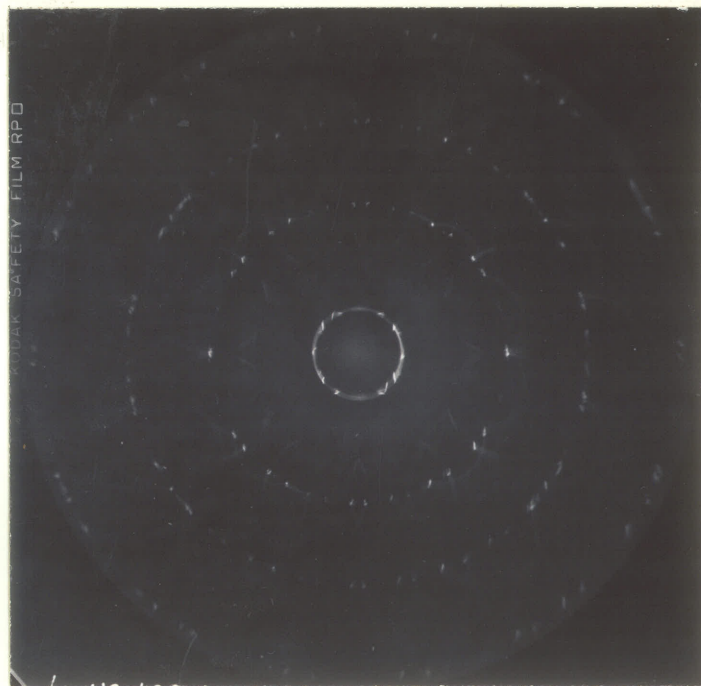


Fig. 10. y-axis, cone-axis photograph of monoclinic wodginite. Natural size, $F=60\text{mm}$, $s=32\text{mm}$, $\bar{\mu}=10^\circ$, MoK_α radiation/Zr filter. Note the few weak reflections which double the b-cell dimension.



they do not mention the strong pseudo-cell in their paper.

Table 3 gives the cell dimensions measured from the precession photographs. The error quoted is the standard deviation of the measurement precision. Within the limits of error the cell dimensions of these specimens have only small differences. The a dimension varies between $9.44^{\pm .02}\text{\AA}$ to $9.51^{\pm .04}\text{\AA}$, b from $11.41^{\pm .02}\text{\AA}$ to $11.44^{\pm .01}\text{\AA}$, c from $5.08^{\pm .01}\text{\AA}$ to $5.12^{\pm .01}\text{\AA}$ and β from $90^{\circ} 25' \pm 16'$ to $91^{\circ} 8' \pm 5'$.

Powder diffractograms of these same specimens were made in the manner described in the previous chapter. Table 4 summarizes the cell dimensions with their standard error for all the unheated wadginites measured on the powder diffractometer. The a and c cell dimensions in these five specimens varies only slightly within the error quoted. The range of β is only $10'$ within the Bernic Lake samples measured here. Table 5 lists the hkl's, estimated intensities and d-values for the Bernic Lake wadginite with the largest β angle and the one with the smallest β angle within the powder patterns of this thesis.

The cell dimensions determined on the powder diffractometer tends to give an average value since unlike the precession method more than one mineral grain is required. The error for the precession cell measurement is approximately 10X that for the diffractometer using the procedures followed here. Several of the cell dimensions

Table 3. Wodginite : Cell dimensions measured from precession photographs

Specimen No.	<u>G69-2</u>	<u>G69-13c</u>	<u>G69-17</u>
a, Å	9.506 [±] .042	9.495 [±] .031	9.436 [±] .021
b, Å	11.408 [±] .020	11.437 [±] .027	11.409 [±] .020
c, Å	5.080 [±] .013	5.075 [±] .013	5.097 [±] .011
β	90° 54' [±] 14'	90° 25' [±] 16'	91° 8' [±] 5'

Specimen No.	<u>G69-39a</u>	<u>BLM-1A</u>
a, Å	9.467 [±] .026	9.503 [±] .013
b, Å	11.439 [±] .014	11.440 [±] .012
c, Å	5.105 [±] .006	5.118 [±] .009
β	90° 33' [±] 15'	90° 40' [±] 12'

Table 4. Cell Dimensions of Wodginites from X-ray Powder

Diffractograms : CuK α radiation/Ni filter,

CaF $_2$ internal standard.

Specimen No.	<u>G69-2</u>	<u>G69-13</u>	<u>G69-17</u>
a, Å	9.496 $^{\pm}$.002	9.497 $^{\pm}$.004	9.517 $^{\pm}$.002
b, Å	11.455 $^{\pm}$.002	11.452 $^{\pm}$.004	11.452 $^{\pm}$.003
c, Å	5.109 $^{\pm}$.001	5.116 $^{\pm}$.002	5.112 $^{\pm}$.002
	91 4.0 $^{\pm}$ 1.9	90 56.2 $^{\pm}$ 2.2	91 5.8 $^{\pm}$ 1.5
V, Å 3	555.64 $^{\pm}$.17	556.39 $^{\pm}$.23	557.00 $^{\pm}$.17

Specimen No.	<u>G69-39</u>	<u>BLM-1A</u>
a, Å	9.498 $^{\pm}$.003	9.498 $^{\pm}$.003
b, Å	11.454 $^{\pm}$.002	11.451 $^{\pm}$.003
c, Å	5.118 $^{\pm}$.001	5.112 $^{\pm}$.002
	90 55.9 $^{\pm}$ 1.8	90 59.4 $^{\pm}$ 1.7
V, Å 3	556.71 $^{\pm}$.16	558.57 $^{\pm}$.20

Table 5. X-Ray Powder Data for Two Wodginites

CuK α radiation/Ni filter, CaF $_2$ internal standard.

Specimen No.		<u>G69-P39</u>		<u>G69-P17</u>	
<u>hkl</u>	<u>I</u>	<u>d(obs.), Å</u>	<u>d(calc.), Å</u>	<u>d(obs.), Å</u>	<u>d(calc.), Å</u>
110	3	7.369	7.311	7.298	7.319
020	5	5.728	5.727	5.732	5.726
200	13	4.758	4.749	4.758	4.758
$\bar{1}11$	4	4.220	4.217	4.214	4.219
111	4		4.168	4.159	4.161
021	4	3.818	3.816	3.810	3.813
220	64	3.658	3.655	3.657	3.659
130	5	3.542	3.542	3.545	3.543
$\bar{2}21$	100	2.993	2.992	2.997	2.996
221	75	2.958	2.957	2.954	2.955
040	17	2.865	2.863	2.865	2.863
002	12	2.559	2.559	2.554	2.555
041	25	2.499	2.499	2.498	2.498
240	2	2.453	2.452		2.453
400	10	2.374	2.374	2.376	2.379
$\bar{2}02$	7	2.266	2.269	2.271	2.269
241	7	2.2028	2.2041	2.2028	2.2030
$\bar{2}22$	5	2.1085	2.1085	2.1096	2.1097
222	5	2.0816	2.0801	2.0802	2.0807
421	5	2.0071	2.0050	2.0063	2.0054
060	6	1.9074	1.9079	1.9079	1.9079
042	6	1.9074	1.9079	1.9079	1.9079
440	7	1.8271	1.8277	1.8290	1.8297
$\bar{3}11$	16	1.7712	1.7712	1.7728	1.7731
260	16	1.7712	1.7712	1.7728	1.7731
$\bar{4}02$	8	1.7542	1.7537	1.7572	1.7580
332	8	1.7542	1.7537	1.7572	1.7580

Table 5. - continued

Table 5. - Continued

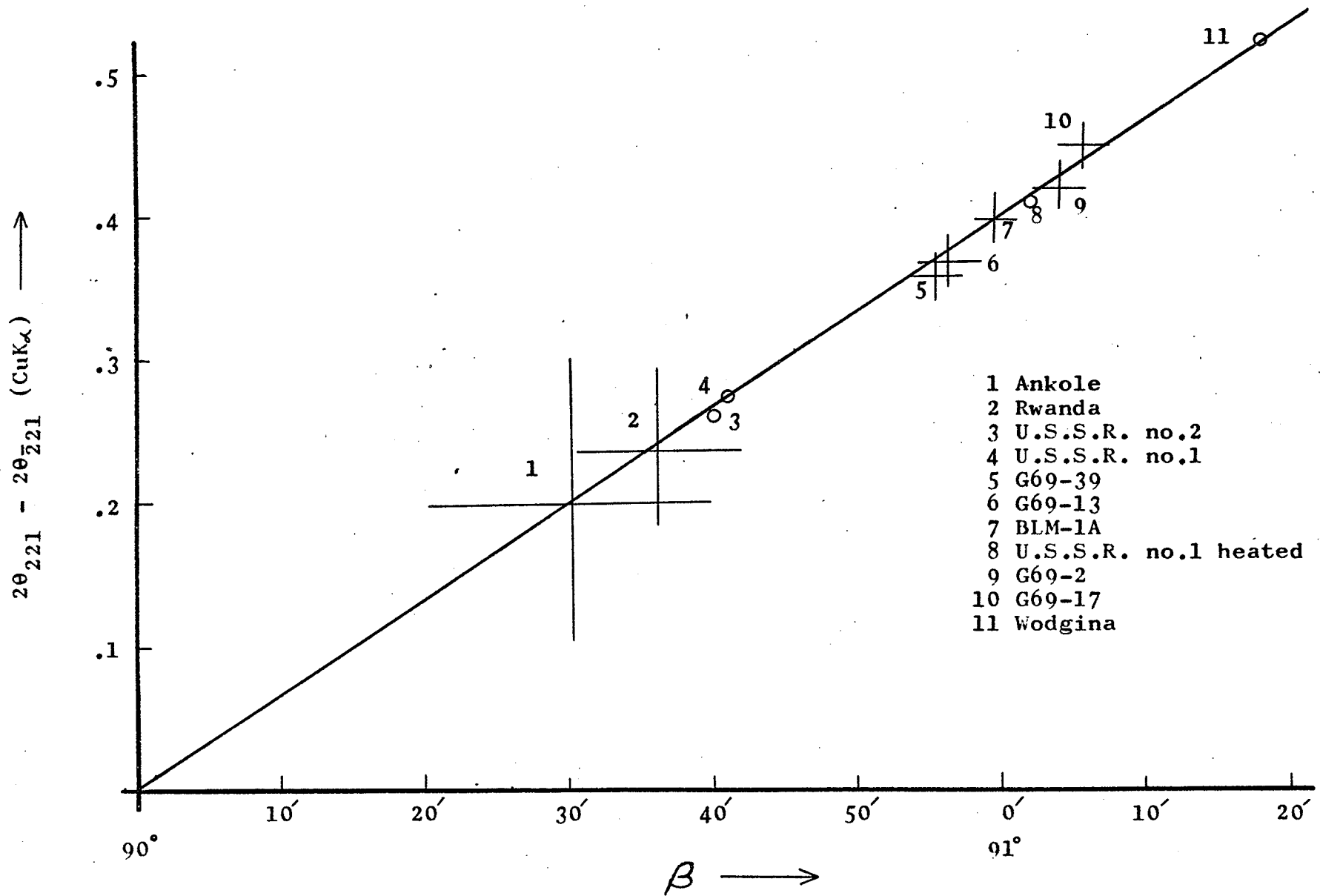
Specimen No.		<u>G69-P39</u>		<u>G69-P17</u>	
<u>hkl</u>	<u>I</u>	<u>d(obs.), Å</u>	<u>d(calc.), Å</u>	<u>d(obs.), Å</u>	<u>d(calc.), Å</u>
402 441	16	1.7274	1.7281	1.7289	1.7307
441	17	1.7141	1.7144	1.7148	1.7146
223 223	15	1.5529	1.5532	1.5536	1.5532
223 171	16	1.5377	1.5383	1.5365	1.5358
521	5		1.4684	1.4721	1.4718
550	2		1.4622	1.4630	1.4637
262	2		1.4604	1.4602	1.4607
370	2		1.4536	1.4533	1.4539
262	2		1.4522	1.4517	1.4510
081	15	1.3785	1.3789	1.3800	1.3784
a		9.498 ± .002 Å		9.517 ± .002 Å	
b		11.454 ± .002 Å		11.452 ± .003 Å	
c		5.118 ± .001 Å		5.112 ± .002 Å	
β		90° 55.9' ± 1.8'		91° 5.8' ± 1.5'	
vol.		556.71 ± .16 (Å) ³		557.00 ± .17 (Å) ³	

measured on the precession photographs (Table 3) are slightly smaller within the limits of error, than those measured by means of the diffractometer (Table 4). This suggests that either the films have stretched or possibly that $F > 60.0$ mm.

Fig. 11 is a graph of β against the splitting of the $\bar{2}21$ and the 221 peaks. All the data presently available from the literature was used by the author on this plot. The $\bar{2}21$ and 221 reflections were chosen since they are the strongest and most easily measured of all the monoclinic splitting pairs. In the paper on the Rwanda material, the β angle was not calculated for the x-ray powder data given. The d-values were thus put into the Appleman et al. computer program and refined as well as was possible for the accuracy of the data given in the paper. The range of the error is indicated on the graph where possible. The plot yields the linear equation:

$$\beta = 90^\circ + \left[149.0 (2\theta_{221} - 2\theta_{\bar{2}21})_{\text{CuK}\alpha} \pm 2\% \right]'$$

Fig.11. Plot of Splitting Between 221 and $\bar{2}21$ Peaks vs β Angle for Wodginites



(f) Heating Experiments

As described in the next chapter the tantalite and pseudo-ixiolite minerals were subjected to heating experiments in order to study the order-disorder relationships between these two minerals. It was decided to heat some wodginite to see if a similar ordering or any other change in the cell took place. Khvostova et al. (1965) found that on heating their wodginite specimen the β angle increased from $90^{\circ} 41'$ to $91^{\circ} 02'$. The present author feels this increase in angle may be related to the degree of oxidation of the elements within the mineral but as of yet this has not been shown to be the case.

Two portions of the same powdered wodginite sample were heated for 16 hours at 1000°C . One portion was heated in an oxidizing atmosphere of pure CO_2 ($f\text{O}_2=10^{-2.5}$ atm). The diffractogram of the product was identical, for all practical purposes, with that of the unheated sample. The oxidized powder retained the light yellow-brown colour it had originally. The other portion was heated in a reducing atmosphere of pure CO ($f\text{O}_2=10^{-17}$ atm). The powder in this case darkened considerably to a brown-black which is characteristic of a reduction in these Ta-oxide minerals. In the x-ray powder diffractograms of the two products, there was no apparent change in the relative

lattice spacings but there were two major changes in intensities. The relative intensity of the 221 peak ($d=2.955\text{\AA}$) increased by a factor of two and that of the 260 peak ($d=1.771\text{\AA}$) increased by a factor of three on heating in pure CO. No attempt has been made by the author to account for these changes. The cell dimensions and standard error for the wadginite heated in the oxidizing and reducing atmospheres are given in Table 6. There is very little difference in cell dimensions; the reduced sample having only a slightly smaller cell.

Table 6. Cell Dimensions of Heated Wodginite Specimen G69-2:

heated at 1000° C for 16 hours, cell dimensions derived from x-ray powder diffractograms, CuK α radiation/Ni filter, CaF $_2$ internal standard.

Atmosphere	fO $_2$ =10 ^{-2.5} atm	fO $_2$ =10 ^{-1.7} atm	Unheated
a, Å	9.491 [±] .002	9.492 [±] .003	9.496 [±] .002
b, Å	11.449 [±] .002	11.452 [±] .003	11.455 [±] .002
c, Å	5.106 [±] .001	5.108 [±] .002	5.109 [±] .001
β	91° 3.7 [±] 1.0'	91° 4.2 [±] 1.8'	91° 4.0 [±] 1.9'
V, Å ³	554.75 [±] .12	555.14 [±] .19	555.64 [±] .17

CHAPTER III. TANTALITE and PSEUDO-IXIOLITE

(a) Introduction

Tantalite is the most commonly known oxide of tantalum. Its relationship to wodginite will be discussed below. The tantalite found at Bernic Lake is Mn-rich and hence it is termed manganotantalite.

Pseudo-ixiolite is applied to disordered tantalite (Nickel et al., 1963b), and such a disordered tantalite is readily ordered by heating for several hours. The pseudo-ixiolite found at Bernic Lake is only partially disordered, but to distinguish it from ordered tantalite the term pseudo-ixiolite is used here. Nickel et al. (1963b) have reserved the term ixiolite for the mineral which has an olovotantalite diffraction pattern on heating. Olovotantalite is a Sn-rich tantalite which is thought to have an orthorhombic cell similar in size to that of wodginite. Matias (1961) was unable to obtain any single-crystal diffraction data.

(b) Physical and Optical Properties

As would be expected, tantalite and pseudo-ixiolite are indistinguishable except by x-ray diffraction methods. At Bernic Lake they form good

crystals, 1 mm. to 10 mm. in size. The crystals are black and the powder is generally dark brown-black. The densities for the five pseudo-ixiolite crystals measured were:

G69-55	6.943	$\pm .025$ gms/cc
G69-58	6.756	$\pm .031$ gms/cc
G69-58	6.599	$\pm .029$ gms/cc
G69-60	6.963	$\pm .032$ gms/cc
G69-61	6.943	$\pm .030$ gms/cc

The low value for both crystals of sample G69-58 are probably due to silicate inclusions. The mean value of the other three determinations is

$$6.950 \pm .029 \text{ gms/cc.}$$

In transmitted light these minerals are opaque with subhedral to euhedral grain outlines. In reflected light they are bright grey (air, blue filter). Under crossed polars they have a dark red-brown internal reflection which almost masks the anisotropism.

(c) Chemistry

Six tantalites and six pseudo-ixiolites were analyzed with the electron probe. The analyses and formulae are given in Table 7. The analysis totals are generally over 100% but not as high as the wodginite totals. This may be due to the fact that the SnO₂ content

Table 7. Semiquantitative Microprobe Analyses of Tantalites

Pseudo-Ixiolites

(a) Tantalite

Analyses in Weight Percent

Specimen No.	G69-81	G69-29BI	G69-29BV	G69-52	G69-S53	G69-S58
MnO	13.7	15.0	14.5	11.3	13.5	14.6
FeO	0.4	0.2	0.4	3.3	0.5	0.2
SnO ₂	0.5	0.1	0.2	0.0	0.7	0.1
TiO ₂	1.5	0.1	0.2	0.2	0.3	0.4
Ta ₂ O ₅	69.3	68.2	70.0	83.5	67.0	64.2
Nb ₂ O ₅	16.0	20.0	17.5	4.0	16.0	21.0
Total	101.4	103.6	102.8	102.3	98.0	100.5

Numbers of Cations on the Basis of 24(O)

Mn ⁺²	3.46	3.71	3.67	3.10	3.58	3.66
Fe ⁺²	.10	.04	.11	.91	.12	.05
Sn ⁺⁴	.06	.02	.02	.00	.08	.61
Ti ⁺⁴	.34	.03	.05	.05	.08	.09
Ta ⁺⁵	5.70	5.41	5.66	7.30	5.71	5.12
Nb ⁺⁵	2.16	2.63	2.38	.62	2.28	2.90
Total	11.92	11.84	11.89	12.08	11.85	11.83

Table 7. - continued

Table 7. - Continued

(b) Pseudo-Ixiolite

Analyses in Weight Percent

<u>Specimen No.</u>	<u>G69-30</u>	<u>G69-31</u>	<u>G69-S55</u>	<u>G69-59</u>	<u>G69-S60</u>	<u>G69-S61</u>
MnO	15.0	15.1	14.4	12.1	14.6	14.4
FeO	0.4	0.5	0.1	4.0	0.1	0.1
SnO ₂	0.2	1.8	0.6	1.2	0.6	0.9
TiO ₂	1.2	1.7	0.8	6.2	0.8	0.6
Ta ₂ O ₅	62.0	64.0	64.0	52.5	64.7	66.2
Nb ₂ O ₅	18.5	18.0	22.0	27.0	21.5	20.5
Total	97.3	101.1	101.9	103.0	102.3	102.7

Numbers of Cations on the Basis of 24(0)

Mn ⁺²	3.93	3.79	3.53	2.51	3.57	3.56
Fe ⁺²	.10	.12	.04	.82	.03	.03
Sn ⁺⁴	.02	.21	.51	1.16	.07	.01
Ti ⁺⁴	.28	.38	.18	1.14	.17	.13
Ta ⁺⁵	5.21	5.15	5.03	3.49	5.08	5.25
Nb ⁺⁵	2.54	2.41	2.95	3.00	2.85	2.72
Total	12.08	12.06	12.24	12.12	11.77	11.70

**Analyst : Mr.S.Jones, Nuclear Research Establishment,
Pinawa, Manitoba.**

is considerably lower in tantalites and pseudo-ixiolites than in wodginites and it was pointed out in the chapter on wodginite that the high totals were thought to be due to abnormally high SnO_2 values. The formula of tantalite is of the type $\text{A}_4\text{B}_8\text{O}_{24}$ where A is Mn and Fe, and B is Ta and Nb. The sites occupied by Sn and Ti are not known, but in tantalites with relatively high Sn and Ti the Ta and Nb are low. This would suggest that when there is considerable Sn and Ti, most are in the B site. The formula of pseudo-ixiolite is of the type A_4O_8 where A is Mn, Fe, Sn, Ti, Ta and Nb. In Table 7 the formula is expressed as $\text{A}_{12}\text{O}_{24}$ to keep it comparable to the tantalite cell.

It was found with the electron probe that these minerals were homogeneous within grains, and fairly consistent in composition in different grains throughout the mine; a notable exception is specimen G69-59 which is higher than the others in TiO_2 and FeO. Generally these minerals are all Mn-rich and Fe-poor. The chemistry of tantalite and pseudo-ixiolite is compared in Chapter V.

(d) Heating Experiments

Pseudo-ixiolite was defined by Nickel et al. (1963b) as a disordered columbite-tantalite. On heating pseudo-ixiolite the structure orders into the A and B sites of tantalite. If these disordered minerals at Bernic Lake had yielded an olovotantalite pattern on heating they would have been termed ixiolites. Four disordered forms were chosen for heating on the basis of their distribution within the mine, and single-crystal and/or powder diffraction patterns were taken of the products after they had cooled to room temperature.

Table 8 lists the specimens heated, the heating conditions, and some general observations of the products after heating. The main difference between the experiments conducted here and those done by Nickel et al. (1963b) or by C. Gouder de Beauregard et al. (1967) was the controlled atmosphere under which the heating took place. Those conducted by the other authors were heated in air whereas the author's were heated in different oxygen fugacities as shown in Table 8.

From these results one can see that the ordering of pseudo-ixiolite to tantalite on heating to these temperatures of approximately 1000° C is apparently not a function of fO_2 . The colour of the powder does seem diagnostic of the oxygen conditions for these mangano-

Table 8. Details of Heating Pseudo-Ixiolites

Specimen No.	Sample	T°C	Hours	fO ₂ atm	Colour after heating	"Ordering"
G69-58	powder	1000	17	10 ^{-14.}	ochre	ordered
G69-58	powder	975	42	10 ^{-15.}	brown-black	ordered
G69-58	powder	995	21	10 ^{-18.}	black	ordered
G69-60	single xl	1000	17	10 ^{-14.}	ochre	ordered
G69-61	single xl	1000	17	10 ^{-14.}	ochre	ordered
G69-61	powder	975	42	10 ^{-15.}	brown-black	ordered
G69-61	powder	995	21	10 ^{-18.}	black	ordered

tantalites, the more reducing the atmosphere the darker being the colour. The unheated powder was a brown-black colour; on heating the powder in an oxidizing atmosphere the colour was ochre and on heating in a reducing atmosphere the powder was black. On the basis of colour changes it would appear these tantalites and pseudo-ixiolites formed in an atmosphere with $fO_2 > 10^{-15}$ atm.

(e) X-ray Diffraction Examination

As has been already mentioned, pseudo-ixiolite and tantalite are closely related crystallographically, the distinction between them being based on the a cell dimension: disordered pseudo-ixiolite has one-third the a dimension of ordered tantalite. On the powder pattern tantalite has peaks at about 7\AA and 5.3\AA whereas pseudo-ixiolite does not (see Fig.25). On heating pseudo-ixiolite these peaks will appear, their intensity being proportional to the degree of ordering.

Seven single crystals were studied from this pair of minerals, four pseudo-ixiolites, two of the same pseudo-ixiolite crystals heated, and one tantalite.

Precession pictures revealed for both minerals:

Diffraction Symmetry:	Orthorhombic	mmm
Extinction Conditions:	hk0	$h+k=2n$
	0kl	$k=2n$
	h0l	$l=2n$
Space Group:	Pbcn	

Figs. 12 and 13 are zero-level, y-axis, precession photographs of a pseudo-ixiolite crystal before and after heating respectively. Even in the unheated material, weak reflections can be seen along x^* suggesting some degree of ordering. These reflections have increased intensities after heating as the degree of ordering increases. Figs. 14 and 15 are x axis cone axis pictures of the same crystal before and after heating. Again it can be seen that after heating, the a-period has been tripled.

A number of powder diffractograms were run on the same specimens. Table 9 gives a complete listing for all the powder data for both a pseudo-ixiolite and a tantalite. From this table one can see that the 200 and 400 reflections of tantalite at 7.2\AA and 3.6\AA respectively are the only really suitable peaks for distinguishing the ordered from the disordered phase. There are other reflections characteristic of tantalite but they are weak and thus often not distinctly recorded. Table 10 is a compilation of the cell dimensions of a number of

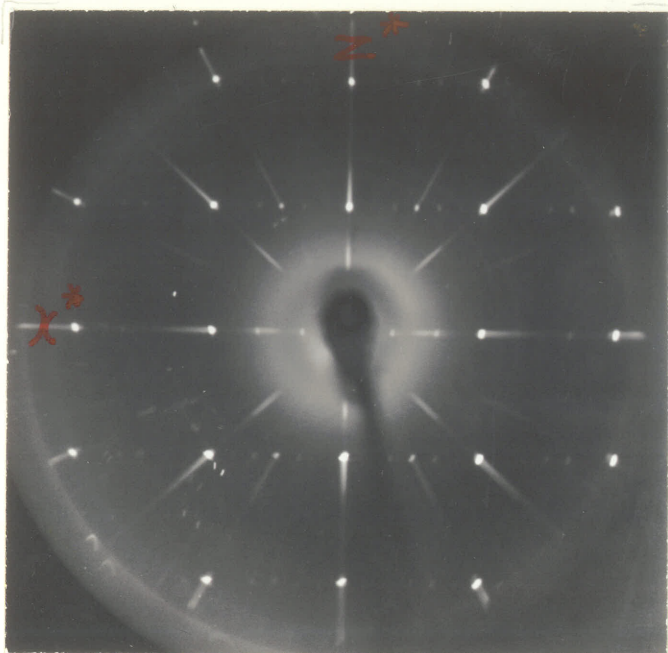


Fig. 12. y-axis, zero-level precession photograph of partially ordered pseudo-ixiolite. Natural size, $F=60\text{mm}$, $\mu=20^\circ$, $\text{MoK}\alpha$ radiation/Zr filter.

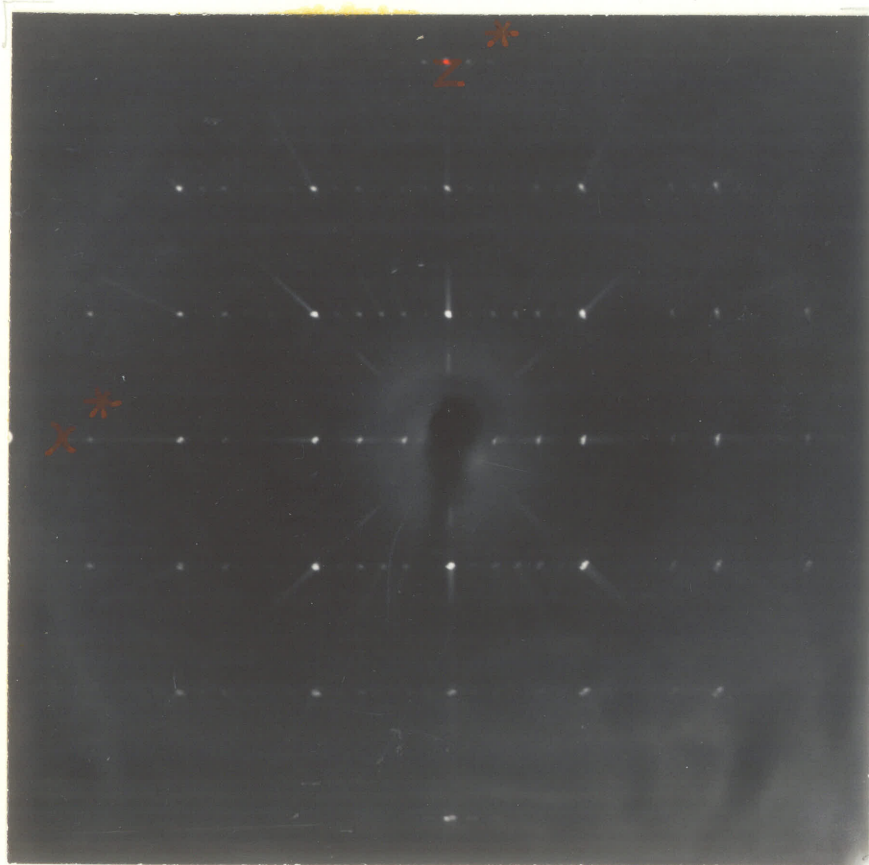


Fig. 13. Same photograph settings as above (except $\mu=25^\circ$) of the same crystal heated. Note the stronger reflections along x^* which triple the a-cell dimension of tantalite.

Fig. 14. x-axis, cone-axis photograph of partially-ordered pseudo-ixiolite. Natural size, $F=60\text{mm}$, $s=32\text{mm}$, $\bar{\mu}=10^\circ$, $\text{MoK}\alpha$ radiation/Zr filter.

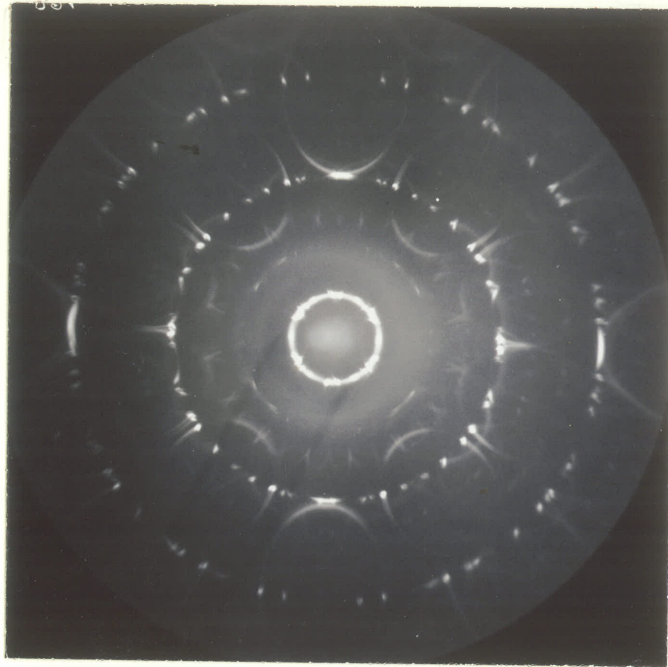


Fig. 15. Same photograph settings as above of the same crystal heated. Note the increased strength of the intermediate levels which triple the a-cell dimension of ordered tantalite.

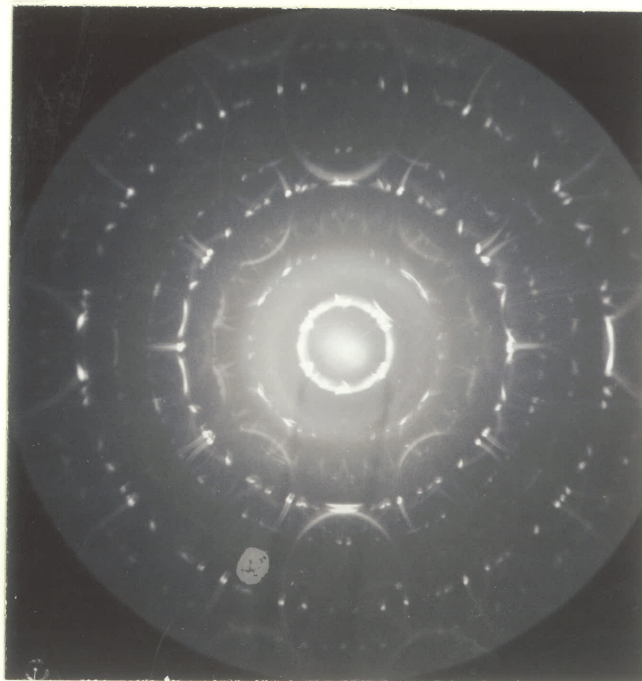


Table 9. X-ray Powder Diffraction Patterns of Pseudo-Ixiolite
and Tantalite : CuK_α radiation/Ni filter, CaF_2
 internal standard.

<u>Pseudo-Ixiolite G69-P61</u>				<u>Tantalite G69-P53</u>			
<u>hkl</u>	<u>I</u>	<u>d(obs.), Å</u>	<u>d(calc.), Å</u>	<u>hkl</u>	<u>I</u>	<u>d(obs.), Å</u>	<u>d(calc.), Å</u>
				200	6	7.227	7.208
				110	4	5.352	5.344
110	30	3.673	3.669	310	35	3.687	3.688
				400	8	3.604	3.604
111	100	2.991	2.990	311	100	2.991	2.992
020	10	2.877	2.877	020	10	2.877	2.877
002	11	2.579	2.579	002	11	2.560	2.558
021	19	2.512	2.513	021	16	2.508	2.508
200	6	2.381	2.381	600	15	2.404	2.403
				420	2	2.247	2.248
112	6	2.110	2.110	312	2	2.102	2.102
				421	3	2.059	2.058
022	8	1.9198	1.9204	022	8	1.9106	1.9116
220	5	1.8340	1.8344	620	6	1.8442	1.8404
				512	8	1.8140	1.8132
				711			
130	19	1.7792	1.7793	330	15	1.7812	1.7813
202	22	1.7490	1.7494	602	20	1.7500	1.7513
221	23	1.7288	1.7284	621	20	1.7333	1.7349
113	8	1.5578	1.5568	313	10	1.5421	1.5420
222	6	1.4953	1.4948	622	5	1.4930	1.4932
311	20	1.4666	1.4670	911	15	1.4763	1.4765
				802	3	1.4708	1.4712
132			1.4645	332	15	1.4600	1.4596
041	3	1.3861	1.3858	041			1.3848
a		4.762 [±] .010 Å				14.416 [±] .009 Å	
b		5.755 [±] .012 Å				5.754 [±] .002 Å	
c		5.158 [±] .013 Å				5.116 [±] .002 Å	
V		141.04 [±] .04(Å) ³				424.39 [±] .29(Å) ³	
Space Group		Pbcn				Pbcn	

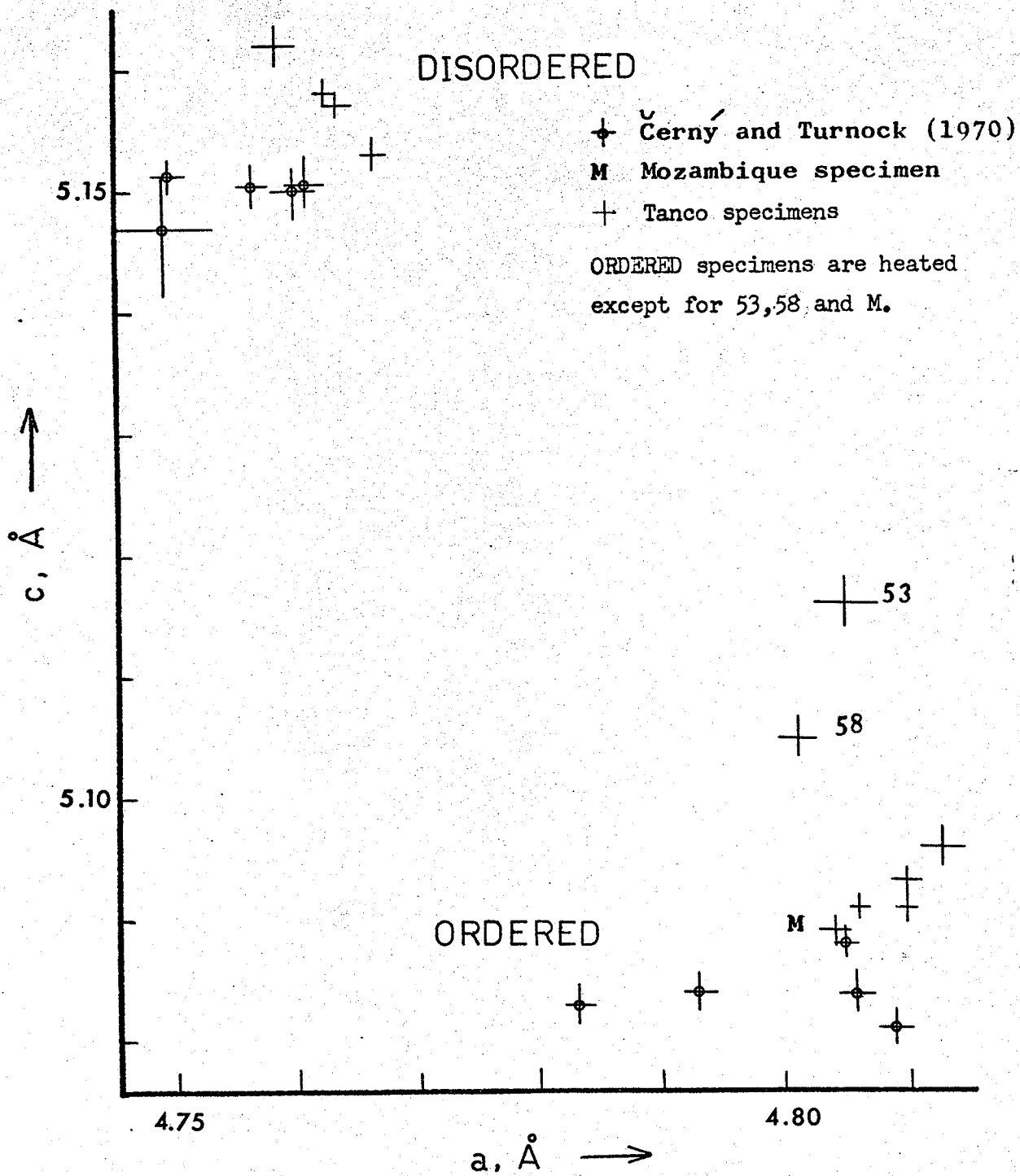
Table 10. Cell Dimensions of Pseudo-Ixiolites and Tantalites
 calculated from x-ray powder diffraction patterns.

Specimen No.	Heated	Ordering	I(200)	a, Å	b, Å	c, Å	v, Å ³
G69-P31	No	disordered	0	4.758 [±] .002	5.750 [±] .002	5.162 [±] .002	141.22 [±] .07
G69-P55	No	disordered	0	4.763 [±] .001	5.753 [±] .001	5.157 [±] .001	141.33 [±] .04
G69-P60	No	disordered	0	4.766 [±] .001	5.753 [±] .002	5.153 [±] .002	141.29 [±] .05
G69-P61	No	disordered	0	4.762 [±] .001	5.755 [±] .001	5.158 [±] .001	141.35 [±] .04
Mozambique	No	ordered		4.804 [±] .001	5.760 [±] .001	5.090 [±] .001	140.89 [±] .04
G69-P53	No	partial	6	4.805 [±] .003	5.754 [±] .002	5.116 [±] .002	141.46 [±] .09
G69-P58	No	partial	11	4.801 [±] .001	5.759 [±] .002	5.105 [±] .002	141.17 [±] .055
G69-PH55	Yes	ordered	11	4.806 [±] .001	5.760 [±] .002	5.091 [±] .001	141.00 [±] .04
G69-PH58	Yes	ordered	14	4.810 [±] .001	5.763 [±] .002	5.091 [±] .001	141.13 [±] .04
G69-PH60	Yes	ordered	10.5	4.810 [±] .001	5.765 [±] .001	5.093 [±] .001	141.25 [±] .03
G69-PH61	Yes	ordered	13.5	4.813 [±] .002	5.765 [±] .002	5.096 [±] .001	141.74 [±] .05

NOTE: $a/3$ for tantalites (ordered)

pseudo-ixiolites and tantalites computed from accurate powder data. The a cell dimension and the volume have been reduced to one-third for the tantalites to make them comparable with pseudo-ixiolite. On ordering, the following changes occur: a increases, b increases slightly, c decreases and the cell volume is approximately constant. Fig. 16, a plot of c versus a shows the marked difference in cell dimensions for ordered and disordered forms. For either form the cell dimensions decrease with increasing iron content (Černý and Turnock, 1970).

Fig.16. Graph of c- versus a-Cell Dimensions for Pseudo-Ixiolites and Tantalites: the a-dimension for tantalite is one-third its true value.



CHAPTER IV RELATED MINERALS WITHIN the TANCO PEGMATITE

(a) Tapiolite

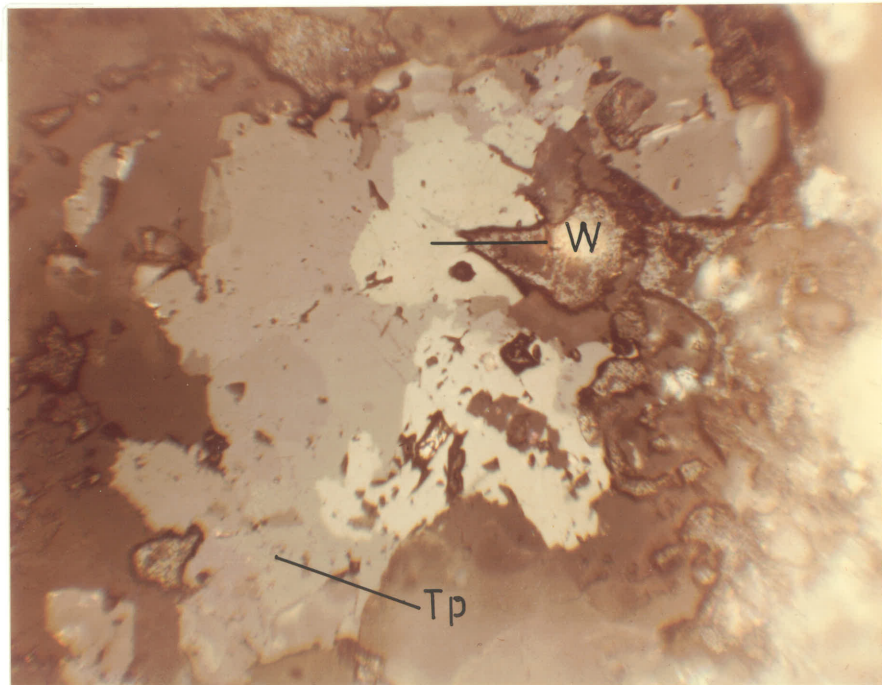
Tapiolite is quite rare in the mine. It is found as small anhedral blebs (Fig. 17) in wodginite or sometimes in tantalite. It can be recognized in polished sections by its weak reflective pleochroism and strong anisotropism. Its reflectivity is very close to that of wodginite and tantalite but the internal reflection is not nearly so marked.

Two semiquantitative electron microprobe analyses are given in Table 11. These analyses are on specimens which are widely separated within the mine yet their compositions are very similar. The formula of tapiolite is of the type $A_2B_4O_{12}$ where A is the metal ions Fe, Mn and possibly Ti and Sn and B is Ta and Nb.

(b) Microlite

Microlite was found in a very few specimens by means of diffractogram patterns or the probe. In the hand specimen or in reflected light, microlite is difficult to distinguish. It is usually fine-grained,

Fig. 17. Tapiolite (Tp) associated with wodginite(W) in partially sericitized K-feldspar. Reflected light, partially crossed polars, X150.



and it resembles yellowish quartz when visible in the hand specimen. In transmitted light, microlite is more readily visible: it is colorless, has a high relief, and is isotropic (Fig. 18).

Microlite is generally closely associated with wodginite, tantalite or pseudo-ixiolite. Often it appears to be of primary crystallization but in some cases it is definitely a replacement mineral (Fig. 19).

Two incomplete semiquantitative probe analyses are given in Table 11. In addition to the oxides listed there the following elements were identified by scanning; major amounts of Ca, and minor amounts of W,U,Si,Cs and Sb. These elements were not determined quantitatively since standards were not available.

(c) Cassiterite

Tin does occur in the form of cassiterite as a separate phase. It is associated with tantalite in the lepidolite zone and in the fine-grained albite bodies. In the wodginite zone, fine-grained cassiterite occurs in fine streaks resembling fracture fillings.

In reflected light the cassiterite has lower reflectivity and less marked internal reflections

Fig. 18. Microlite (M) associated with wodginite (W) in partially sericitized K-feldspar. Transmitted light, plane polarized, X60.

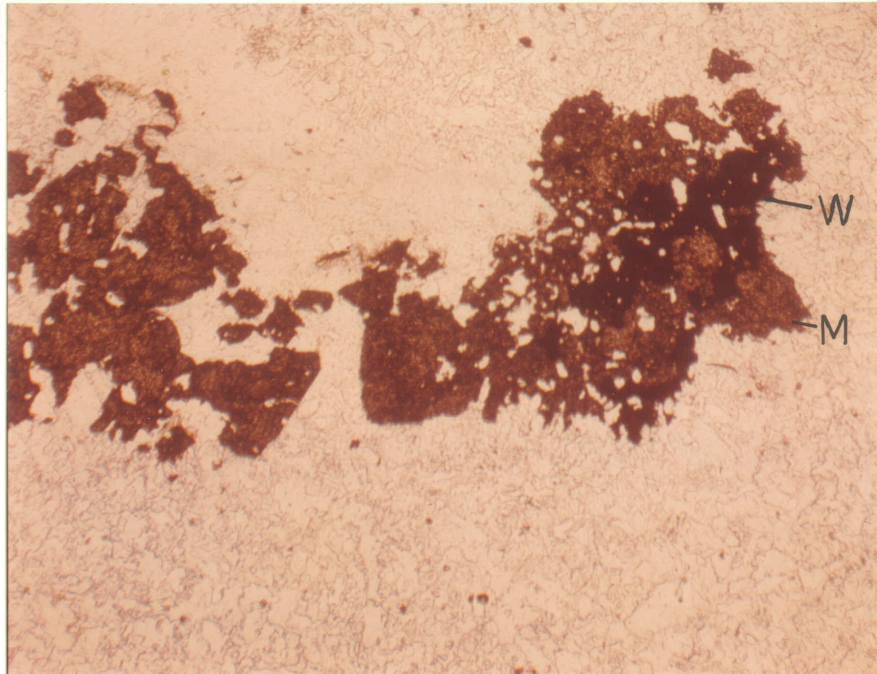
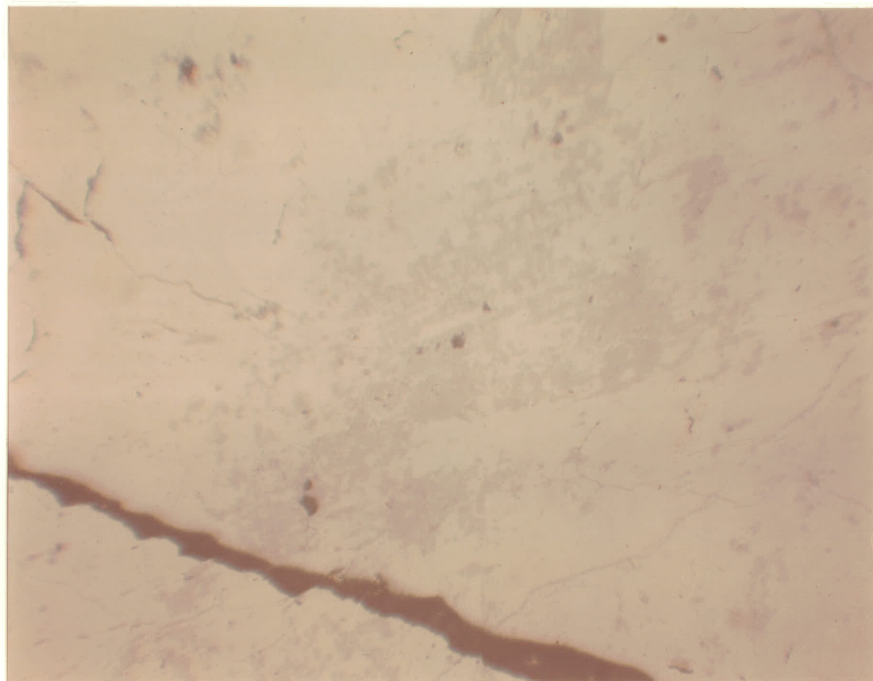


Fig. 19. Microlite replacing pseudo-ixiolite. [Matrix minerals are quartz and feldspar.] Reflected light, plane polarized, X150.



than tantalite (Fig.20). Under the probe electron beam cassiterite was luminescent.

Microprobe analyses indicated that the cassiterite contains up to 3% Ta_2O_5 or Nb_2O_5 and minor amounts of TiO_2 and FeO.

(d) Ilmenite

Although no ilmenite was found in the samples collected by the author in the mine, some was separated from the shaker table concentrates using the Frantz Isodynamic Separator (separation and identification by A.C.Turnock).

This concentrate was then analysed by atomic absorption and x-ray fluorescence methods (see Table 11). The Fe is expressed as total FeO. Usually in ilmenites about one-half the iron is Fe_2O_3 , and if this were so in the analysis the total would come close to 100%. Due to the abundance of MnO in this ilmenite the mineral should be termed manganilmenite.

Fig. 20. Cassiterite (C) grain in tantalite. Reflected light, plane polarized, X75.

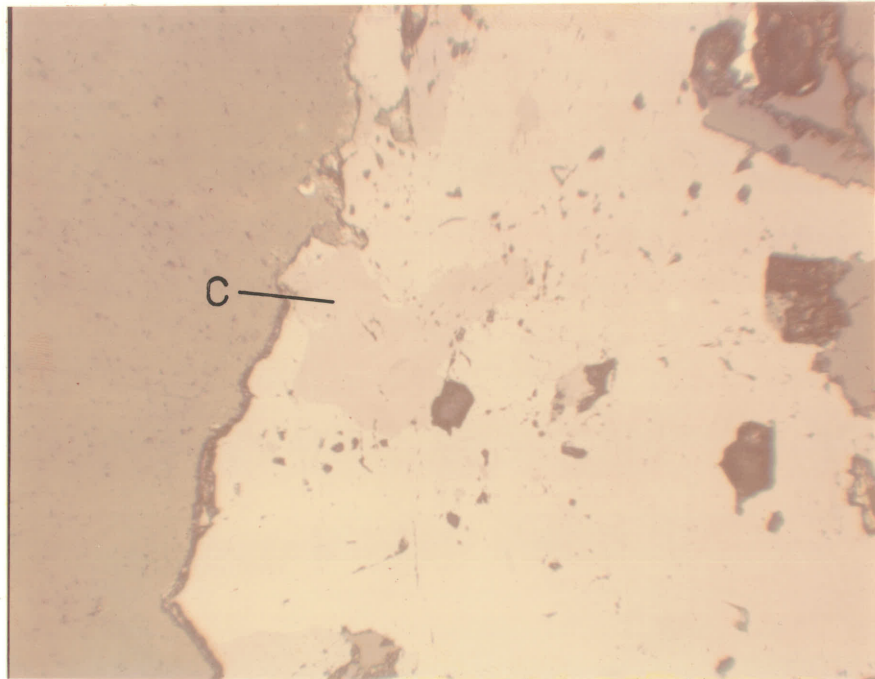


Table 11. Analyses of Some of the Related Minerals

Analyses in Weight Percent

Specimen No.	<u>Tapiolites</u>		<u>Microlites</u>		<u>*Ilmenite</u>	
	G69-21	G69-52	G69-30	G69-31		
FeO	13.5	14.0	0.5	0.5	FeO	36.
MnO	2.1	2.2	0.8	0.7	TiO ₂	51.
SnO ₂	0.2	0.2	0.5	0.2	MnO	9.1
TiO ₂	0.2	0.1	1.0	1.0	MgO	0.5
Ta ₂ O ₅	85.0	85.0	73.	74.	Al ₂ O ₃	tr.
Nb ₂ O ₅	2.4	2.2	6.0	5.5	SiO ₂	0.0
Total	103.4	103.7	81.8	81.9	Total	96.6

Numbers of Cations on the Basis of 12(O)

Fe ²⁺	1.83		1.90	
Mn ²⁺	.29		.30	
Sn ⁴⁺	.01	2.16	.01	2.22
Ti ⁴⁺	.03		.01	
Ta ⁵⁺	3.75		3.79	
Nb ⁵⁺	.18	3.93	.17	3.96
Total	6.09		6.18	

**Analyst: Mr. S. Jones; electron microprobe analyses,
Nuclear Research Establishment, Pinawa, Manitoba.**

***Analyst: The author; atomic absorption and x-ray
fluorescence analysis, University of Manitoba.**

CHAPTER V. RELATIONSHIPS BETWEEN THE Ta-OXIDES
IN THE TANCO PEGMATITE

(a) Chemical Relationships

The chemical distinction between wodginite on the one hand and tantalite and pseudo-ixiolite on the other, is quite marked. The ternary plot in Fig. 21 shows that wodginite has considerably more ($\text{SnO}_2 + \text{TiO}_2$), less ($\text{Ta}_2\text{O}_5 + \text{Nb}_2\text{O}_5$), and slightly less ($\text{FeO} + \text{MnO}$) than either tantalite or pseudo-ixiolite. The chemical differences between tantalite and pseudo-ixiolite are not so great. Tantalites except for sample G69-8I have lower ($\text{SnO}_2 + \text{TiO}_2$) and higher ($\text{Ta}_2\text{O}_5 + \text{Nb}_2\text{O}_5$) than pseudo-ixiolites. The ($\text{FeO} + \text{MnO}$) is in the same range for both. Sample G69-8I contained tantalite and wodginite together in bluish aplite. Specimen G69-59 contains considerably more SnO_2 and TiO_2 than the other pseudo-ixiolites.

Fig. 22 is a graph of FeO/MnO ratio vs $\text{Ta}_2\text{O}_5/\text{Nb}_2\text{O}_5$ ratio. Since ratios are being used here the scale was arbitrarily chosen to vary from 0/1 to 1/0 and divided into (8) equal parts. Wodginites have higher Ta/Nb ratios and generally have higher Fe/Mn ratios than tantalites or pseudo-ixiolites. An exception to this is specimen G69-52, a tantalite which plots near the wodginite specimens. This specimen is associated with

Fig. 21. Ternary Plot of ($Ta_2O_5 + Nb_2O_5$), ($SnO_2 + TiO_2$), and ($FeO + MnO$)
in Weight Percentages for Tanco Specimens

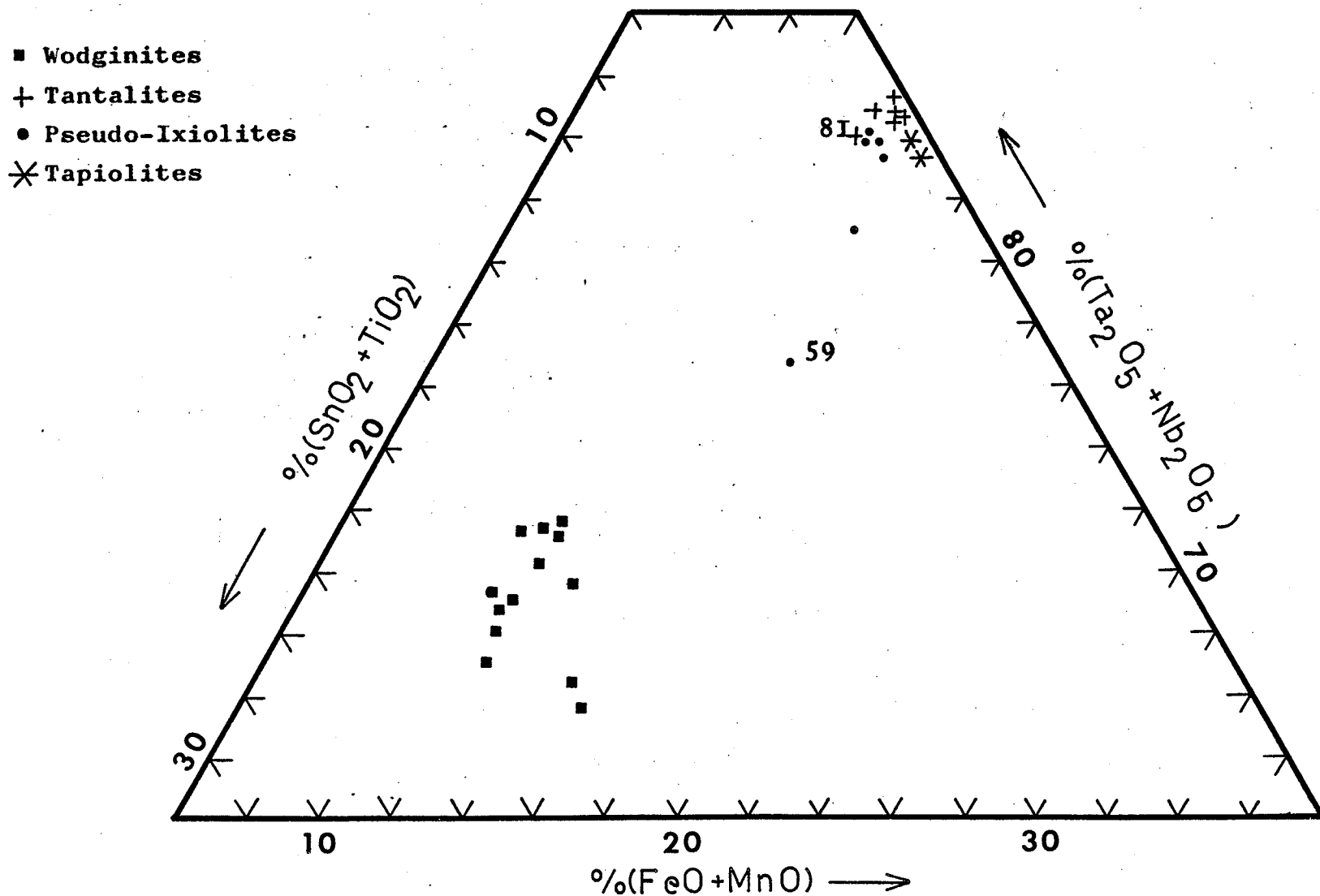
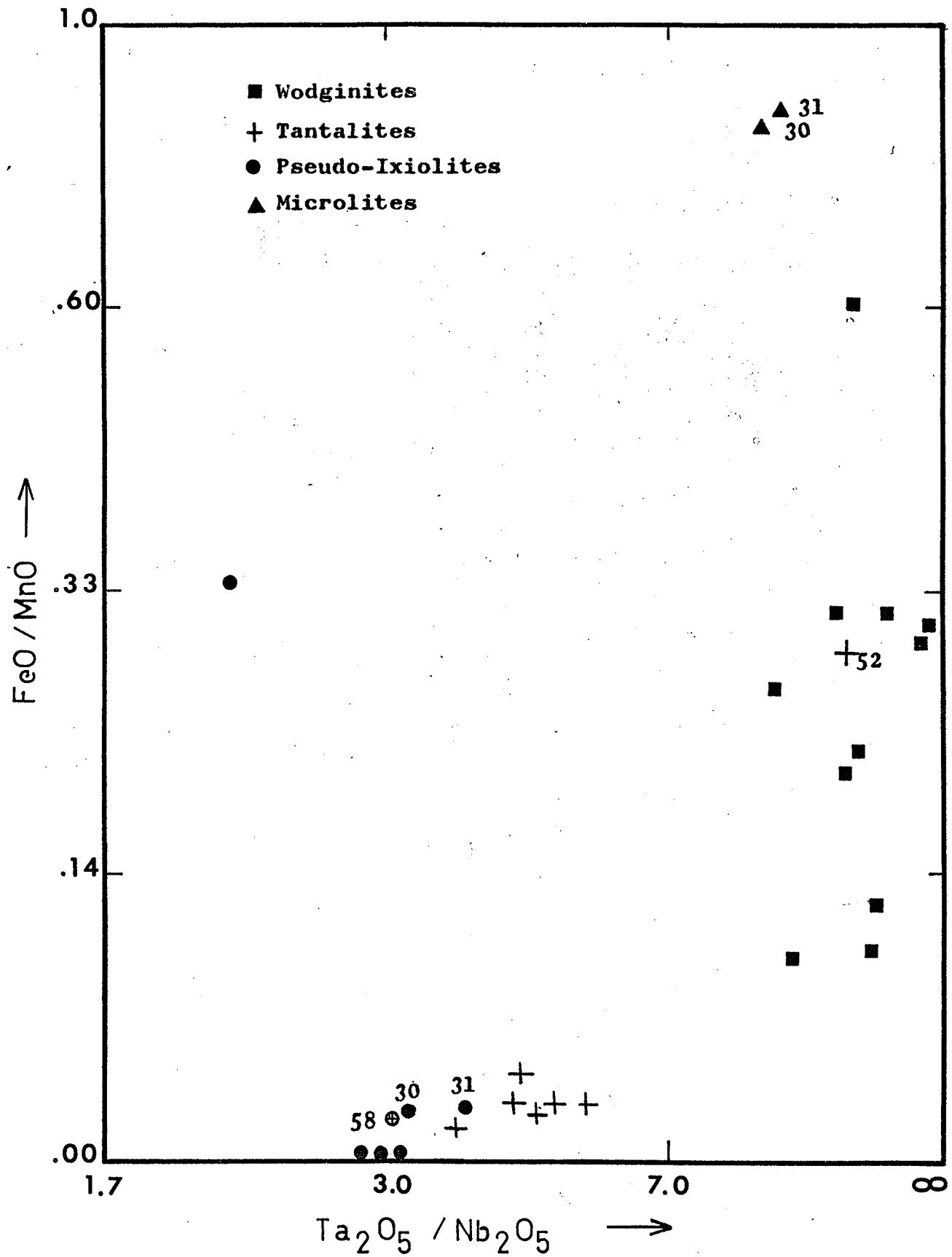


Fig.22. Weight Percent Ratios of FeO/MnO versus Ta_2O_5/Nb_2O_5 for Wodginite, Tantalite, Pseudo-Ixiolite and Microlite Specimens from the Tanco Pegmatite



tapiolite and tapiolite has a Fe/Mn ratio much higher than wodginites and a Ta/Nb ratio in the same range as wodginites in this pegmatite. In general the tantalites have slightly higher Ta/Nb ratios than the pseudo-ixiolites. Specimens G69-30 and G69-31 are pseudo-ixiolites which are approaching the Ta/Nb ratios of the tantalites. The Ta/Nb ratio of these specimens may have been affected by partial replacement by microlite; it can be seen in Fig.22 that microlite has a considerably higher Ta/Nb ratio than pseudo-ixiolites. Another specimen of interest on this graph is G69-58. This specimen was collected in the quartz-plagioclase-spodumene zone (zone 1) adjacent to the aplitic albite (zone 3). In the final chapter the geological setting of the various Ta minerals will be discussed but it should be pointed out here that specimen G69-58 has the chemistry and geological environment characteristic of pseudo-ixiolites but is in fact partially ordered. This may be due to some influence of the adjacent zone 3 which characteristically contains ordered tantalites.

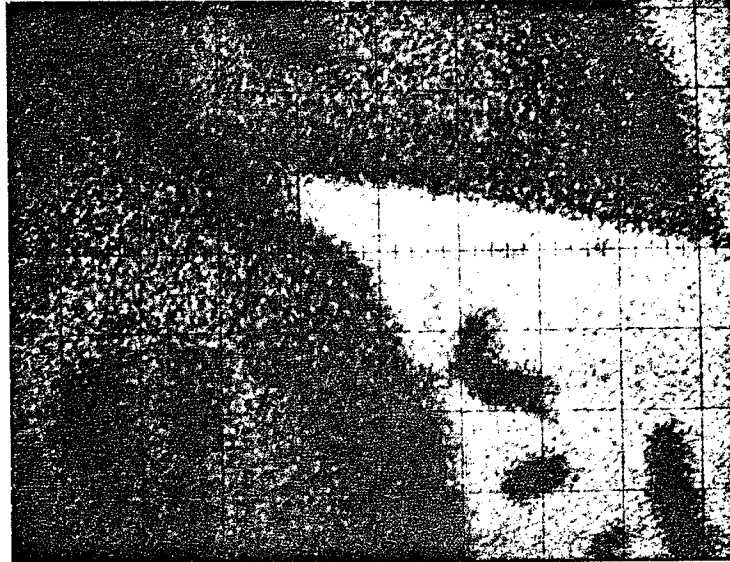
Specimen G69-29b was a large sample of aplitic albite with tantalite similar to that shown in Fig.27. From this specimen five polished sections were made and a crystal probed in each. The sections were along a line with G69-29bV being furthest from the quartz-aplite contact and section G69-29bI closest to the contact;

presumably the tantalites in section G69-29bV would be the first to crystallize. The Ta_2O_5/Nb_2O_5 ratios for these sections were (I) $3.4^{+0.3}$, (II) $4.5^{+0.3}$, (III) $4.9^{+0.3}$, (IV) $4.6^{+0.3}$, and (V) $4.0^{+0.3}$. It can be seen there was no regular variation in the Ta/Nb ratio for crystallization on this small of a scale (the specimen was approximately eight inches across).

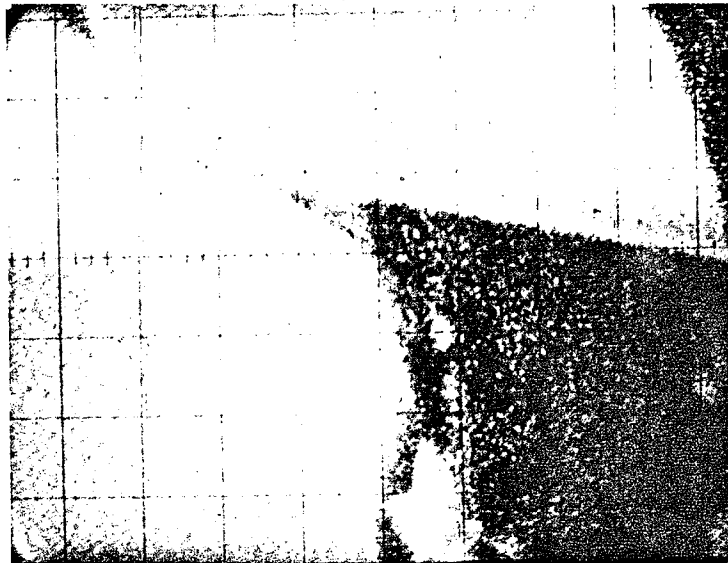
Although Turnock (1963) has shown that Sn is not an essential constituent in synthesizing wodginite, Fig. 21 shows that the Sn definitely prefers the wodginite structure to that of tantalite or pseudo-ixiolite. Sn must have been present when the tantalites were crystallizing since cassiterite and tantalite have crystallized together (see Fig.20) yet even when these two minerals are intimately associated very little Sn enters the tantalite structure (see x-ray scans Fig.23).

Fig.24 shows the relationship of the cell volume to the weight ratio $(FeO + TiO_2 + SnO_2)/MnO$ for wodginites, tantalites and pseudo-ixiolites (using the ixiolite cell to make them all directly comparable). The cell volume decreases as the $(FeO + TiO_2 + SnO_2)/MnO$ ratio increases for all three minerals. In tantalites and pseudo-ixiolites where the TiO_2 and SnO_2 contents are high the trend may not hold since Sn and Ti may substitute for Ta and Nb in these minerals. Two examples of this are specimens GL-9-19 and GL-9-20 (Černý and

Fig. 23. Electron microprobe x-ray scanning images. Cassiterite grain (left) adjacent to a tantalite grain. Note the very small amount of Sn in the tantalite.



Ta -Scan



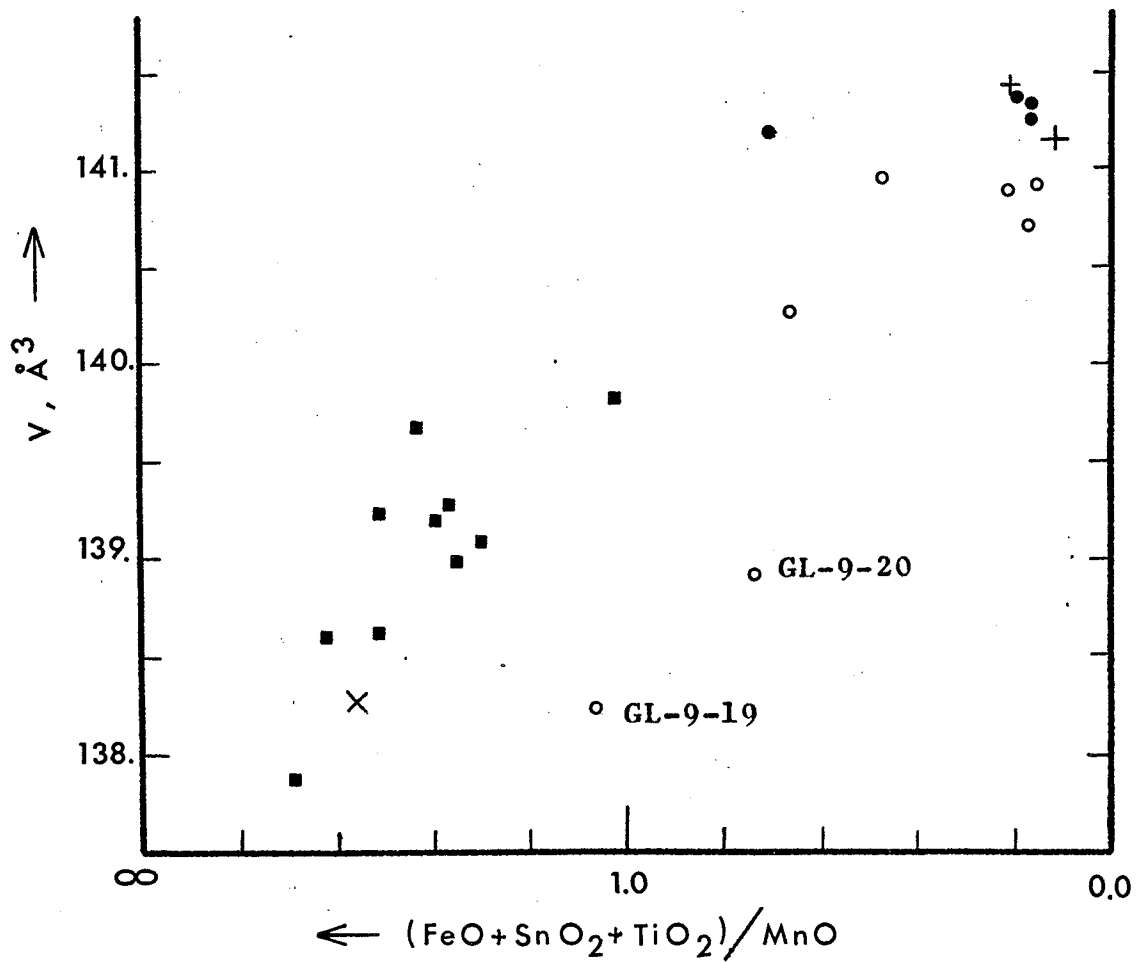
Sn-Scan

50 μ

Fig.24 Cell Volumes (Ixiolite Cell) versus Weight Ratios
(FeO + SnO₂ + TiO₂)/MnO for Wodginites, Tantalites
and Pseudo-Ixiolites

- Wodginites
- + Tantalites
- Pseudo-Ixiolites

- Černý and Turnock (1970)
- X Tantalites
 - Pseudo-Ixiolites



Turnock, 1970). The explanation for this trend is that the Mn^{2+} ion has a larger ionic radius than either Fe^{2+} , Fe^{3+} , Ti^{4+} or Sn^{4+} .

Goldschmidt's Ionic Radii in Å

Fe^{2+}	.83	Sn^{4+}	.74
Fe^{3+}	.67	Ti^{4+}	.64
Mn^{2+}	.91		

Thus as the Mn^{2+} content increases the cell volume increases.

(b) Crystallographic and Structural Relationships

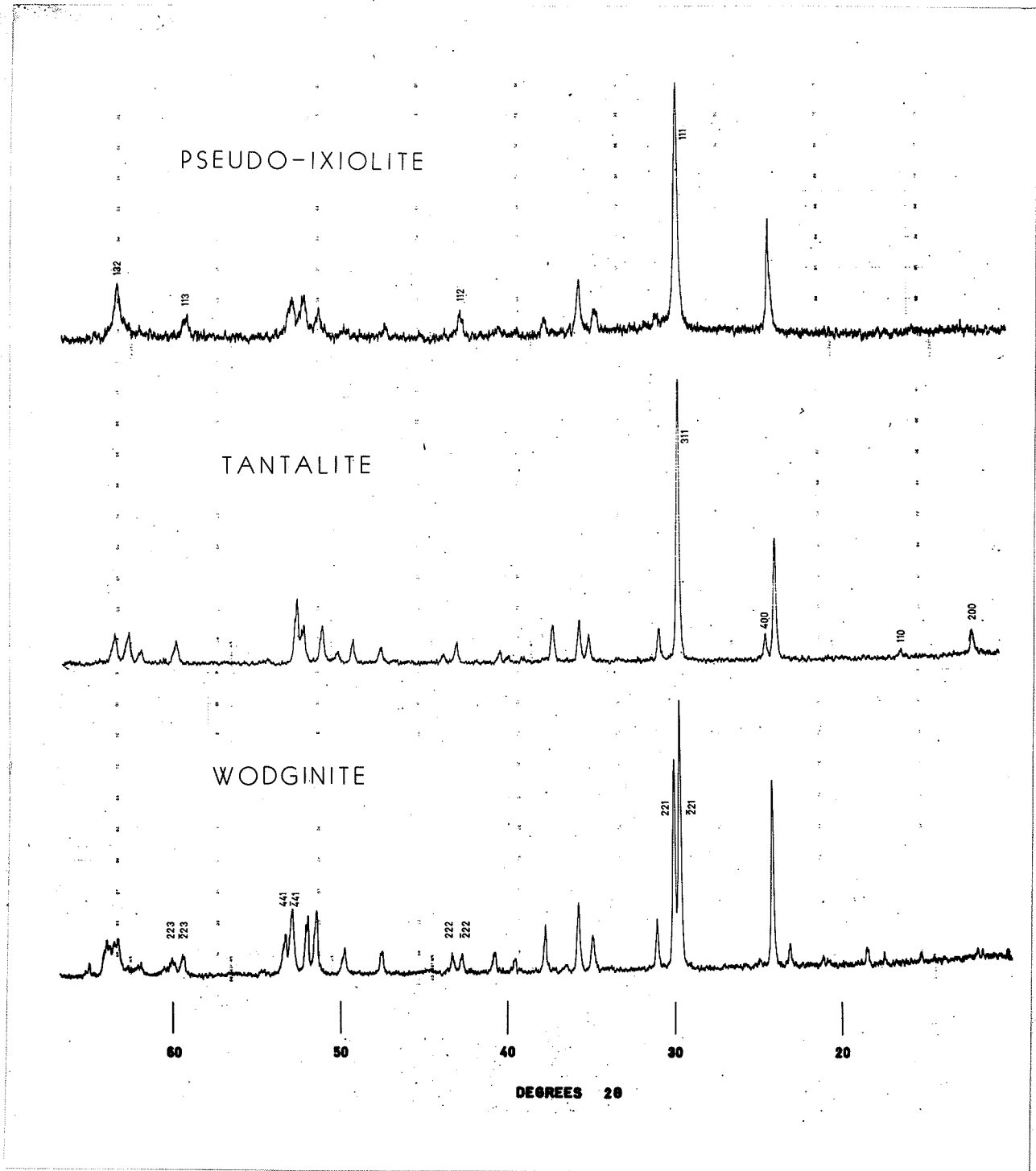
Tantalite, pseudo-ixiolite and wodginite are all very closely related crystallographically. In this thesis these three minerals have been referred to common axes according to Strunz and Tennyson (1966), the determining setting being that of monoclinic wodginite with β obtuse and $c < a$ (see Table 12). The settings used in the paper by Nickel et al. (1963a) are also given in Table 12 for comparison.

To emphasize the crystallographic similarities of these three minerals, powder diffractograms of pseudo-ixiolite, tantalite and wodginite, all from the Tanco mine, are shown in Fig. 25. Tantalite is an ordered pseudo-ixiolite, and on ordering the a-period is tripled. Some of the additional peaks of ordered tantalite relative to

Table 12. Orientation Settings of Ixiolite, Tantalite and Wodginite

	Strunz et al.(1966) and this thesis			Nickel et al.(1963a)	
	Ixiolite	Tantalite	Wodginite	Ixiolite	Tantalite
Axial Lengths, Å	a=4.76 b=5.75 c=5.16	a=3x4.80 b=5.76 c=5.10	a=2x4.76 b=2x5.73 c=5.10	c=4.74 b=5.73 a=5.15	b=3x4.75 a=5.73 c=5.08
β Angle	(90°)	(90°)	91°	(90°)	(90°)
Cell Volume, (Å) ³	141	3x141	4x139	140	3x138
Space Group	Pbcn	Pbcn	C 2/c or Cc	Pnab	Pcan

Fig. 25. X-ray powder diffractograms of pseudo-ixiolite, tantalite and wodginite, all from the Tanco pegmatite. $\text{CuK}\alpha$ radiation/Ni filter, scanning speed of one-half degree per minute.



pseudo-ixiolite can be seen on the diffractogram in Fig.25; 200 at $12.3^{\circ} 2\theta$, 110 at $16.6^{\circ} 2\theta$, 400 at $24.7^{\circ} 2\theta$, 512 or 711 at $50.3^{\circ} 2\theta$, and 802 at $63.1^{\circ} 2\theta$. Wodginite gives an even more complex pattern than tantalite because of the doubling of both the a - and b - periods relative to a and b in pseudo-ixiolite, and because of the lowering to monoclinic from orthorhombic symmetry. Additional peaks in wodginite due to doubling of a - and b - periods are, 110 at $12.1^{\circ} 2\theta$, $\bar{1}11$ at $21.1^{\circ} 2\theta$, 111 at $21.3^{\circ} 2\theta$, and 130 at $25.1^{\circ} 2\theta$. (Note that where h and k indices are odd in wodginite there is no possibility of a corresponding reflection in pseudo-ixiolite.) Examples of peak splitting due to the monoclinic distortion of the pseudo-ixiolite cell are; 111 into $\bar{2}21$ and 221 at $30^{\circ} 2\theta$; 112 into $\bar{2}22$ and 222 at $43^{\circ} 2\theta$; 221 into $\bar{4}41$ and 441 at $53^{\circ} 2\theta$; 113 into $\bar{2}23$ and 223 at $60^{\circ} 2\theta$; and 132 into $\bar{2}62$ and 262 at $64^{\circ} 2\theta$.

Since the structure of wodginite has not yet been determined, the reason for the monoclinic distortion of the ixiolite cell is not yet known. One might suspect that any parameter which influenced the size of the β angle may be related to the ixiolite-wodginite transformation. Von Knorring et al. (1968) attributed the increase in β to an increase in Mn/Fe ratio, yet when the author plotted $\frac{t}{\lambda}$ all available data of this type no satisfactory conclusions can be made as to the effect of Fe and Mn on the β angle. Furthermore there is no sound

pseudo-ixiolite can be seen on the diffractogram in Fig.25; 200 at $12.3^{\circ} 2\theta$, 110 at $16.6^{\circ} 2\theta$, 400 at $24.7^{\circ} 2\theta$, 512 or 711 at $50.3^{\circ} 2\theta$, and 802 at $63.1^{\circ} 2\theta$. Wodginite gives an even more complex pattern than tantalite because of the doubling of both the a - and b - periods relative to a and b in pseudo-ixiolite, and because of the lowering to monoclinic from orthorhombic symmetry. Additional peaks in wodginite due to doubling of a - and b - periods are, 110 at $12.1^{\circ} 2\theta$, $\bar{1}11$ at $21.1^{\circ} 2\theta$, 111 at $21.3^{\circ} 2\theta$, and 130 at $25.1^{\circ} 2\theta$. (Note that where h and k indices are odd in wodginite there is no possibility of a corresponding reflection in pseudo-ixiolite.) Examples of peak splitting due to the monoclinic distortion of the pseudo-ixiolite cell are; 111 into $\bar{2}21$ and 221 at $30^{\circ} 2\theta$; 112 into $\bar{2}22$ and 222 at $43^{\circ} 2\theta$; 221 into $\bar{4}41$ and 441 at $53^{\circ} 2\theta$; 113 into $\bar{2}23$ and 223 at $60^{\circ} 2\theta$; and 132 into $\bar{2}62$ and 262 at $64^{\circ} 2\theta$.

Since the structure of wodginite has not yet been determined, the reason for the monoclinic distortion of the ixiolite cell is not yet known. One might suspect that any parameter which influenced the size of the β angle may be related to the ixiolite-wodginite transformation. Von Knorring et al. (1968) attributed the increase in β to an increase in Mn/Fe ratio, yet when the author plotted ^t all available data of this type no satisfactory conclusions can be made as to the effect of Fe and Mn on the β angle. Furthermore there is no sound

crystal-chemical reason for any variation of β with these chemical parameters. In the tantalite series there is a wide variation in Fe and Mn contents. The variation in the amount of either of these elements is reflected in the cell dimensions but $\beta = 90^\circ$ is not altered. The author also tried to relate the β angle variation found in this work and other publications with various other chemical parameters, but none yielded a satisfactory solution to the problem. In his study of the Fe-Mn-Ta-O system Turnock (1966) found that wodginite formed at oxygen fugacities greater than $10^{-9.0}$ atm whereas below this oxygen fugacity, tantalite formed as the stable Mn-rich phase and tapiolite as the stable Fe-rich phase. Since this transformation from orthorhombic tantalite to monoclinic wodginite is dependent on oxygen fugacity so might the β angle also be related to the degree of oxidation of the elements present. This was indicated on page 39 where it was pointed out that when Khvostova et al. (1965) heated their wodginite, presumably in air, the β angle increased. Unfortunately the oxidation states of the Fe and Mn in the analyses done here and elsewhere are unknown, and no actual relationship between β and oxygen pressure formation can be stated yet.

CHAPTER VI. GEOLOGICAL IMPLICATIONS

Within the portion of the pegmatite which was sampled, wodginite, tantalite and pseudo-ixiolite occur in different zones. Wodginite occurs mainly in the K-feldspar-muscovite-plagioclase-quartz-beryl zone immediately below the quartz core. Its environment is often as shown in Fig.26 where coarse dark-coloured quartz is adjacent to beryl and the ore is in the coarse feldspar usually associated with green or yellow muscovites. Pseudo-ixiolite occurs in the quartz-plagioclase-K-feldspar-spodumene-muscovite zone just outside of the wodginite-bearing zone. The pseudo-ixiolite forms good crystals generally on albite-quartz grain boundaries, and in places there is minor greenish-muscovite present. Tantalite and some wodginite occur in the bluish aplite which occurs mainly towards the base of the pegmatite and in small patches in other parts of the pegmatite. The concentration of the Ta-oxides increases upwards towards the contact with the other pegmatite zones (Fig.27), indicating their late crystallization within the aplite. The tantalites and wodginites found in the aplite are fine-grained and are interstitial amongst albite crystals (Fig. 28).

The occurrence of wodginite and pseudo-ixiolite in separate zones within the pegmatite might be attributed to wodginite having crystallized at a higher fO_2 than

Fig. 26. Wodginite (W) in typical K-feldspar (K-f)-
quartz (Q)-beryl(B) environment, (Zone 2).

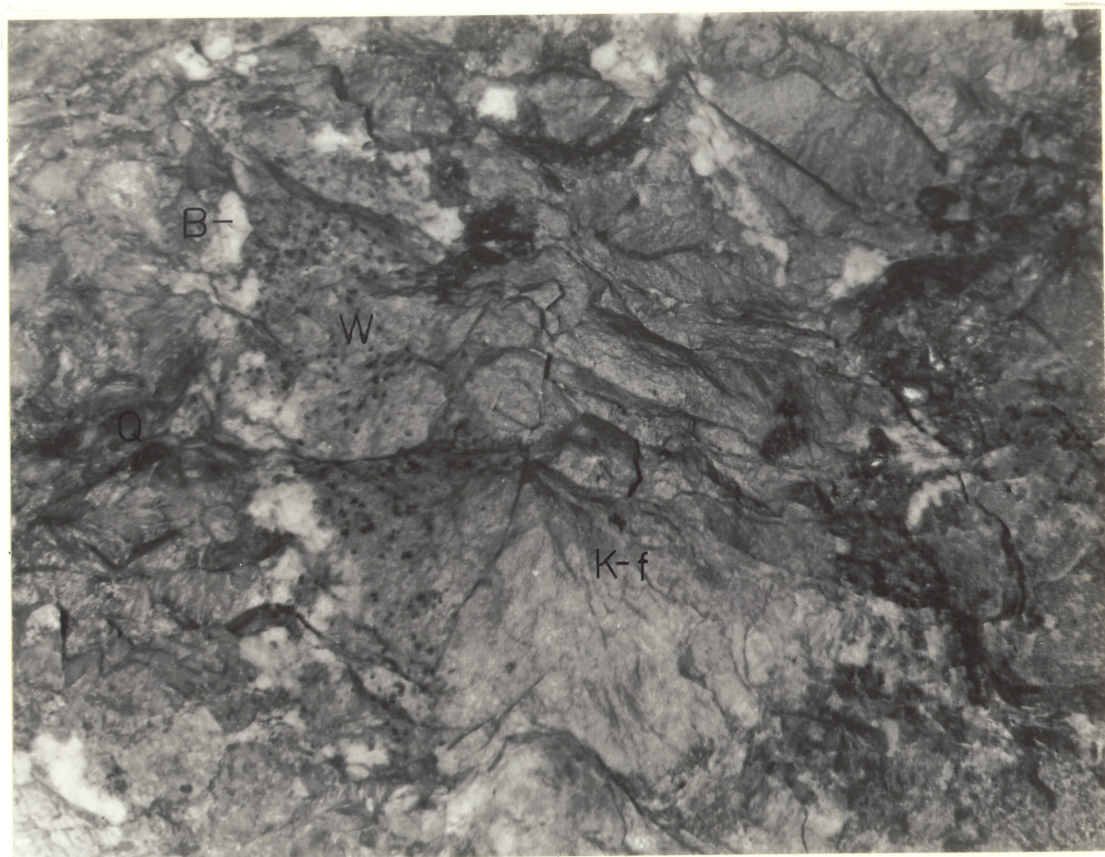


Fig. 27. Tantalite (T) and possibly wodginite in aplitic albite (Ap) near quartz(Q) contact, (Zone 3).

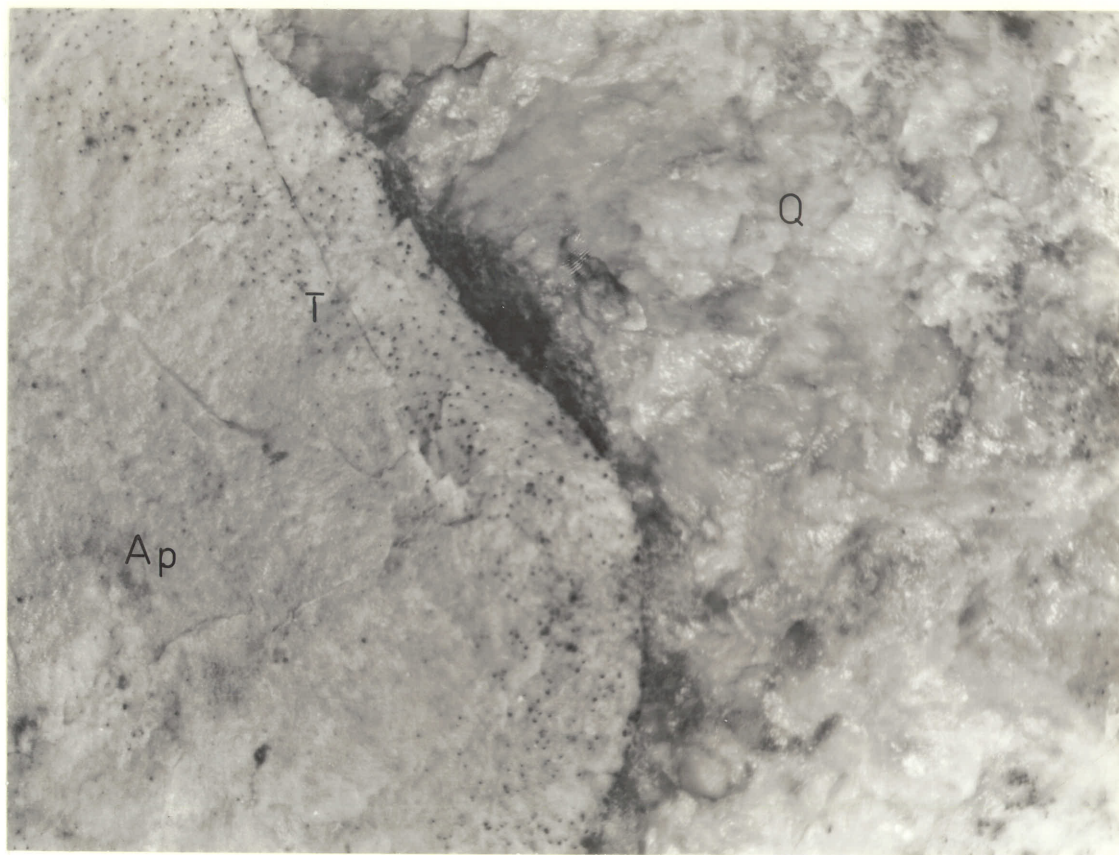


Fig. 28(a). Interstitial tantalite grain in aplitic albite.
Transmitted light, plane polarized, X80.

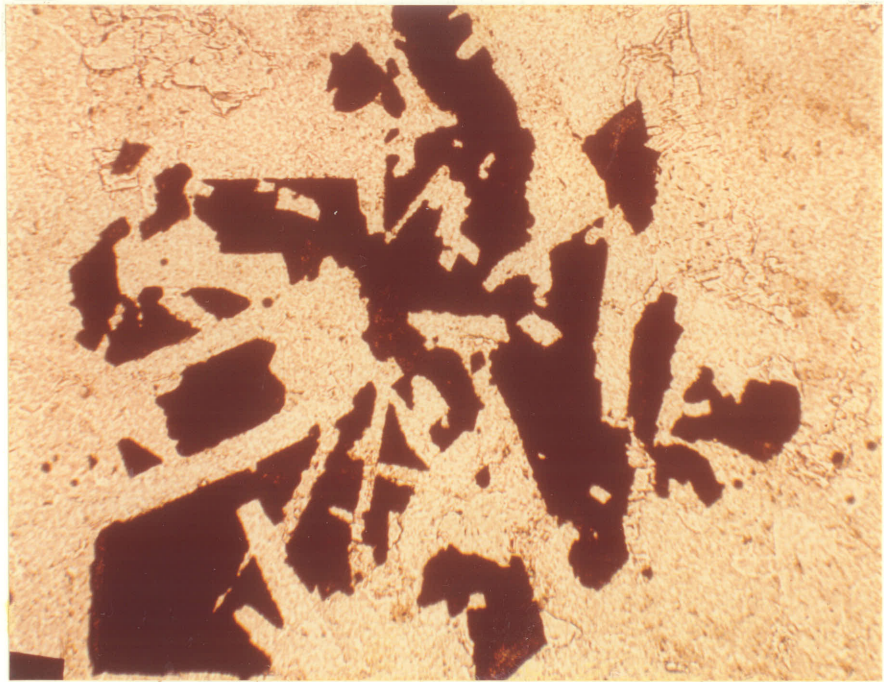
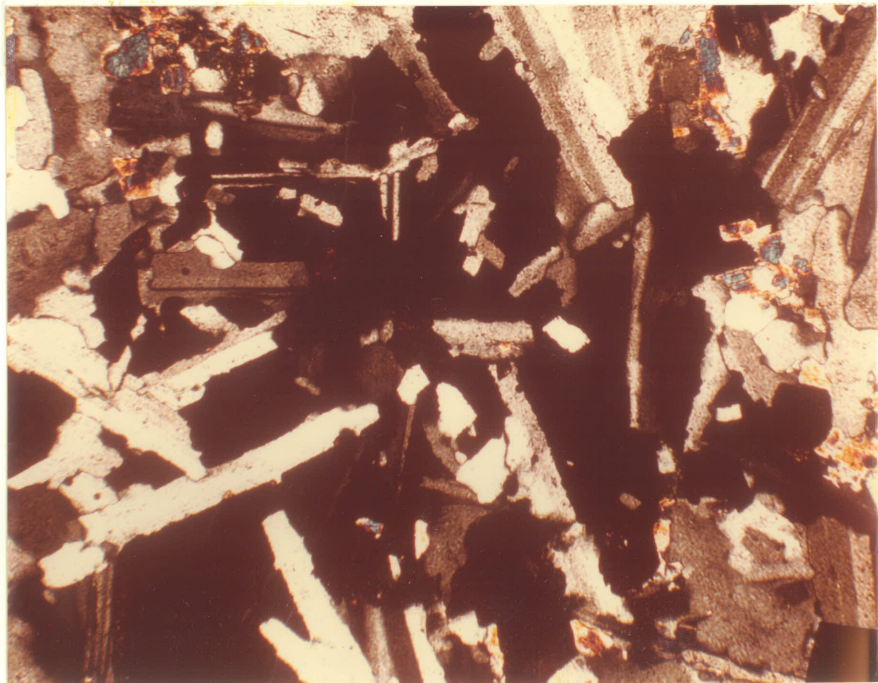


Fig. 28(b). Same tantalite grain as in Fig. 28(a) showing
cross cutting albite crystals. Transmitted
light, crossed polars, X80.



pseudo-ixiolite (Turnock, 1966). This increase in fO_2 could be a consequence of increasing water pressure upon crystallization. The wodginite-bearing zone being closer to the core of the pegmatite than the pseudo-ixiolite-bearing zone has presumably crystallized later and consequently at higher P_{H_2O} . The bluish albitic aplite appears to have a Ta mineralogy that is distinctive from the other zones in that it contains both tantalite and wodginite; this suggests an fO_2 compatible with the crystallization of both of these minerals. Jahns and Burham (1969) suggested that in pegmatites of this type the albitic aplite is a primary zone, formed early in the sequence of pegmatite crystallization. If this is true the slightly higher Ta/Nb ratios of the tantalites in the early aplite over those of pseudo-ixiolite in a later zone is consistent with the ideas of Fersman (1940) and Kornetova (1961), whereby the first tantalites to crystallize in a Ta-rich pegmatite have higher Ta/Nb ratios.

REFERENCES

- APPLEMAN, D.E., HANDWERKER, D.S. and EVANS, H.T. (1963): Least squares refinement of crystal unit cell with powder diffraction data by an automatic computer indexing method. United States Geological Survey.
- BOURGUIGNON, P. et MELON, J. (1965): Wodginite du Rwanda. Ann. Soc. Geol. de Belgique, t. 88, p.291 - 300.
- ČERNÝ, P. and TURNOCK, A.C. (1970): Niobium-Tantalum Minerals from Granitic Pegmatites at Greer Lake, Southeastern Manitoba. Can. Min., in print.
- FERSMAN, A.E. (1940): Pegmatites. Selected Works v.6, Publishing House of the Academy of Sci. of U.S.S.R. Moscow 1960.
- JAHNS, R.H. and BURNHAM, C.W. (1969): Experimental Studies of Pegmatite Genesis. Econ. Geol., v.64, p.843-864.
- GOUDER DE BEAUREGARD, C., DUBOIS, J. et BOURGUIGNON, P. (1967): Comportment Thermique des Columbotantalites. Ann. Soc. Geol. de Belgique, t.90, Bull. no 4-6.
- HUTCHINSON, R.W. (1959): Geology of the Montgomery Pegmatite. Econ. Geol., v.54, p.1525-1542.
- KHVOSTOVA, V.A., PAVLOVA, V.N., ALEKSANDROV, V.B. and MAKSIMOVA, N.V. (1965): The First Find of Wodginite in the U.S.S.R. (Translation). Dokl. Acad. Sci. U.S.S.R., Earth Sci. Sect., v. 167, p. 109-112.
- von KNORRING, O. (1968): On the geochemistry of some niobium-tantalum minerals from African pegmatites. 12th Ann. Rept. Inst. African Geol., Univ. Leeds, p.50-53.
- von KNORRING, O., SAHAMA, T.G. and LEHTINEN, M. (1969): Ferrous Wodginite from Ankole, South-West Uganda. Bull. Geol. Soc. Finland 41, p. 65-69.
- KORNETOVA, V.A. (1961): Some observations on the Columbite-Tantalite Mineral Group. Transaction of the Min. Museum of the Acad. Sci. U.S.S.R. v.12 p.36-53.
- LUNA, J. (1965): Wodginite and columbite-tantalite from a pegmatite at Krašovice (Western Moravia). Acta Univ. Carolinae, Geologica No.3, p.157.

- MATIAS, V.V. (1961): Olovotantalite, a New Variety of Tantalite. Geol. Mestorozhd. Red. Elem. v.9, p.30-41.
- NICKEL, E.H., ROWLAND, J.F., and McADAM, R.C. (1963a): Wodginite- a new tin manganese tantalite from Wodgina, Australia and Bernic Lake, Manitoba. Can. Min., v.7, p.390-402.
- NICKEL, E.H., ROWLAND, J.F., and McADAM, R.C. (1963b): Ixiolite- a columbite substructure. Amer. Min., v.48, p.961-979.
- RUCKLIDGE, J.C. and GASPARRINI, E.L. (1969): EMPADR VII- a computer program for processing electron microprobe analytical data. Univ. Toronto.
- SMITH, F.G. (1969): Personal communication.
- STRUNZ, H. and TENNYSON, C. (1966): Mineralogische Tabellen, 4. Aufl. Akad. Verl. Ges. Leipzig.
- STURDIVANT, J.H. (1930): The Crystal Structure of Columbite. Z. Krist. v.75, p.88-108.
- TILLING, R.I. (1968): Zonal distribution of variations in structural state of alkali feldspar within the Rader Creek Pluton, Boulder Batholith, Montana. J. of Pet., v.9 #3.
- TURNOCK, A.C. (1966): Synthetic wodginite, tapiolite and tantalite. Can. Min., v.8, p. 461-469.
- VORMA, A., SIIVOLA, J. (1967): Sukulaite - $Ta_2Sn_2O_7$ - and wodginite as inclusions in cassiterite in the granite pegmatite in Sukula, Tammela in SW Finland. C.R. Soc. geol. Finlande, No.39, p.173-187.
- WRIGHT, C.M. (1963): Geology and Origin of the Pollucite-Bearing Montgarry Pegmatite, Manitoba. Geol. Soc. of Am. Bull., v.74, p. 919-946.